310/1749-8

ICTP-COST-CAWSES-INAF-INFN
International Advanced School
on
Space Weather
2-19 May 2006

_____

Circulation in the Equatorial Middle Atmosphere

Kevin Peardon HAMILTON
Professor and Chair
Department of Meteorology, and
International Pacific Research Center (IPRC)
University of Hawai`i at Manoa
Honolulu, HI 96822
USA

Notes on the Circulation in the Equatorial Middle Atmosphere

Kevin Hamilton

May 6, 2006

1. Introduction

There are a number of features that distinguish the the dynamics of the tropical stratosphere and mesosphere from the dynamics elsewhere in the atmosphere.

1. The small Coriolis parameter at low latitudes leads to a breakdown of the validity of the geostrophic approximation for the wind and invalidates the quasi-geostrophic theory that is so useful in explaining the large-scale circulation of the extratropical atmosphere. Another consequence of the small Coriolis parameter is that temperature observations (e.g. from satellite radiometers) are of limited use in inferring winds at low latitudes. Thus it is much harder in the tropics to diagnose the detailed dynamics from available observations, leading to more reliance on indirect theoretical and modelling approaches to study the general circulation.

2. The mean temperature structure in low latitudes is quite distinctive. Fig. 1 shows idealized temperature vs. height plots appropriate for the midlatitudes and for the equator. The equatorial region is notable for having higher temperatures in the lower troposphere and a colder/higher tropopause than is seen at higher latitudes. The height-latitude section of zonal-mean temperature in April determined from climatological observations is shown in Fig.2. The temperatures near the equatorial tropopause are extremely cold with observations ∼190K.

3. The mean temperature structure combined with the the extremely nonlinear dependence of water vapor mixing ratio have important implications for the dynamics and chemistry of the atmosphere. In the lower and mid-troposphere the warm tropical temperatures and high water vapor mixing ratios lead to the possibility of very strong latent heat release. When combined with the small Coriolis parameter this can lead to strong convectively-driven, strongly-divergent motions. At higher latitudes much more of the forcing of weather systems comes from con-

version of potential energy associated with north-south temperature gradients.

Moist convection and precipitation have strong peaks near the equator. Fig. 3 shows the annual-mean precipitation estimated from observations. The low-latitude peak of rainfall is evident in this picture, but at a particular time the narrow meridional concentration of convection is even more pronounced. Over the oceans the convection is concentrated in the Intertropical Convergence Zone (ITCZ), which moves north and south following the sun through the year. As we will see, the time-variation of tropical convection excites vertically-propagating waves that are crucial to the dynamics of the tropical stratosphere.

4. The very cold temperatures in the tropical stratosphere are accompanied by extremely dry conditions. Fig. 4 shows the observed zonal-mean water vapor mixing ratios in the upper troposphere and lower stratosphere. The strong gradients near the tropopause are evident. Also noteworthy are the very small values throughout the stratosphere, particularly above the height of the equatorial tropopause, what has come to be called the "overworld". The implications of this dryness for the atmosphere (and indeed human life) is profound. With little water, the chemistry of the stratosphere is very different from the troposphere - there are no clouds (except in winter at very high latitudes), no precipitation, and much lower concentration of OH radical which catalyzes much of the homogeneous chemistry in the lower atmosphere.

Explaining the extremely dry conditions in the overworld seems possible only if it assumed that all the air entering the overworld enters through the equatorial tropopause. Fig. 5 shows a schematic of the large-scale circulation of the troposphere. There are many issues now being researched relating to how the air actually gets into the stratosphere and exactly what determines how dry it is. However, it seems clear that any changes in the equatorial tropopause temperature

will result in changes in the stratospheric water vapor, with important implications for stratospheric ozone chemistry. Interestingly, there is now considerable evidence of a rising trend in stratospheric water vapor. Fig. 6 shows the trend in annual mean water vapor concentration during 1981-2000 determined from balloon observations at Boulder (40N). So far there seems to be no clear connection of this trend with tropopause temperatures, but concerns about stratospheric chemistry response to tropospheric climate change represents one of the key practical reasons for studying the detailed dynamics of the equatorial middle atmosphere.

5. Perhaps the most distinctive features of the circulation in the neutral tropical middle atmosphere are the large-amplitude, long-period oscillations seen in the zonally-averaged flow. In particular, the winds and temperatures of the equatorial stratosphere undergo a very strong quasi-biennial oscillation (QBO) while the region from near the stratopause to the lowermost thermosphere displays a prominent semiannual oscillation (SAO). Fig. 7 shows a height-time section of monthly-mean zonal wind near 8N during 1962-1966 put together from balloonsonde measurements at Balboa (9N) to 30 km, and rocketsonde measurements from 30-56 km. This figure is strikingly different from the result one would obtain from higher latitude stations. Notably the annual (12-month) harmonic would dominate any higher latitude plot, but it is almost absent in this near-equatorial section. Instead, in the lower stratosphere the variation in wind seems to be interannual, while in the upper stratosphere there is a variation with period of 6 months.

In the lower stratosphere, say 16-35 km, the observations show a systematic variation from westerly (*eastward*) to easterly (*westward*) roughly every other year. In a later lecture we will look at observations of this phenomenon in much longer data records. We will see that it has a variable period that averages about 28 months, leading to the term "quasi-biennial oscillation" (QBO) to describe it.

4

The QBO is a fascinating feature of the circulation, and is the closest thing to an internally-generated periodic phenomenon in the general circulation, to be contrasted with the genuinely periodic (and astronomically forced) diurnal and annual cycles. The QBO is much more regular than other widely-studied quasi-periodic phenomena in the atmosphere-ocean system, such as the Southern Oscillation or North Atlantic Oscillation.

The existence of the QBO demonstrates another way in which the tropical middle atmosphere is unique. The QBO is so regular that the winds in the tropical stratosphere are predictable months, and even years, in advance. The normal expectation based on tropospheric and midlatitude experience is that purely atmospheric phenomena have a limit of practical predictability of 2-3 weeks at most. The enhanced predictability of the tropical stratospheric wind is associated with the ability of the momentum in the zonally-averaged flow in this region to act as an effective long-term "memory" for the atmospheric circulation. In the next section of these notes we will try to explain the physics behind this phenomenon.

6. The equatorial atmosphere is also characterized by unique electrodynamic phenomena. The terrestrial geomagnetic equator is shown in Fig. 8 along with the geomagnetic latitude lines defined relative to this equator. The ionosphere displays fascinating phenomena that seem largely confined to low geomagnetic latitudes just as the neutral atmosphere has phenomena restricted to near the geographical equator. One early observation was that solar diurnal variations in the magnetic field tend to be enhanced near the geomagnetic equator. This has been attributed to the effects of a narrow ionospheric current confined near the geomagnetic equator and termed the "equatorial electrojet". See Forbes (1981) for a review.

2. Basic Dynamical Considerations - The "Radiative Spring"

While not perfectly monochromatic, the equatorial QBO is the most spectacular example of a quasi-periodic oscillation in the atmosphere that is not astronomically forced (such as the annual and diurnal cycles). The QBO has a time-scale of deterministic predictability of months or even years - in strong contrast to meteorologists' usual picture of predictability in the atmosphere. An attempt will be made to explain this surprising feature within the simplest possible contexts. We will first consider the mean flow response to eddy forcing and show why the circulation in the equatorial region is likely to behave quite differently from that in higher latitudes. Then in a later lecture we will treat the very simple case of two internal gravity waves interacting with the mean-flow, to illustrate how long-period oscillatory equatorial mean-flow variations may be produced.

Governing Equations and Notation

We will assume a basic knowledge of the equations (momentum, continuity, thermodynamic, equation of state) governing fluid motion on a rotating sphere. Derivations can be found in standard textbooks such as Holton (1992). To study the large-scale circulation it is often useful to make the "primitive equation" approximations, replacing the vertical momentum equation by hydrostatic balance and considering only the Coriolis effects associated with the component of the earth's rotation vector parallel to the local vertical (termed the "Coriolis parameter", $f = 2\Omega \cos(\theta)$).

We will adopt "standard" meteorological notation where u, v, w represent the zonal, meridional and vertical components of the winds, with westerly (eastward), southerly (northward), and upward velocities defined as positive. Location is de-

fined by coordinates θ, the latitude, ϕ, longitude (east as positive) and z, the geometrical height above the earth's surface. Fig. 10 shows a schematic of this coordinate system.

In many instances it it convenient to approximate the full spherical geometry by planar geometry, indeed several different "flavours" of this kind of approximation are useful. In a simple instance we will be considering models of the equatorial flow that ignore rotation and replace the zonal direction by Cartesian direction, x, with an assumption of periodic boundary conditions in this direction. Another approach, the so-called "f-plane" retains the Coriolis force, but with a constant value of the Coriolis parameter, f. Finally, the equatorial region is often treated with an "equatorial β-plane", in which the Coriolis parameter is taken to depend linearly on the meridional distance from the equator, $f=\beta y$.

The decay of mean atmospheric density with height has important implications for many aspects of atmospheric dynamics. However, it also introduces complications in the mathematical treatment of the equations. In some instances it is useful to make one further assumption, familiar to oceanographers, namely the Boussinesq approximation. In the Boussinesq approximation the atmospheric density is treated as constant except in the hydrostatic equation (where varying density affects the horizontal gradients of pressure which drive the circulation). For quantitative results in the atmosphere, the Boussinesq approximation is almost always inadequate, but - if the system studied is hydrostatic - some of the mathematical simplification of the Boussinesq approximation can be retained in the compressible equations by transforming the vertical coordinate from geometrical height to something proportional to the logarithm of pressure. We will discuss these "log-pressure" coordinates later.

Zonal Mean and Eddies

For many purposes it is useful to divide the atmospheric circulation into its zonal-mean component and all deviations from the zonal-mean (which we refer to as the "eddy" component). Thus, for example, the zonal wind can be written as

$$u = \overline{u} + u'$$

where the overbar refers to an average around a latitude circle (or equivalently over the full x-domain in a Cartesian geometry model).

The separation between the zonal-mean and eddy components can be applied to the governing equations. Consider, for example, the zonal momentum equation in the very simple 2D (x-z) Boussinesq case:

$$\frac{\partial u}{\partial t} = -u\frac{\partial u}{\partial x} - w\frac{\partial u}{\partial z} - \frac{1}{\rho_o}\frac{\partial P}{\partial x}$$

where P is the pressure and ρ_o is the (constant) mean density. Substituting the zonal-mean, eddy decomposition and then averaging over x yields an equation for the rate of change of the zonal-mean zonal wind:

$$\frac{\partial \overline{u}}{\partial t} = -\overline{w}\frac{\partial \overline{u}}{\partial z} - \overline{w'\frac{\partial u'}{\partial z}}$$

the Boussinesq version of the continuity equation is

$$\frac{\partial u}{\partial x} + \frac{\partial w}{\partial z} = 0$$

When averaged over x the continuity equation implies that

8

$$\overline{w} = 0$$

and

$$\frac{\partial u'}{\partial x} + \frac{\partial w'}{\partial z} = 0$$

This can then be used to rewrite the zonal-mean momentum equation in the familiar form

$$\frac{\partial \overline{u}}{\partial t} = -\frac{\partial \overline{u'w'}}{\partial z}$$

Here the acceleration of the mean flow is forced by the effect of the eddies which can be regarded as a convergence of a "Reynolds stress" or "vertical eddy flux of zonal momentum". It emphasizes the role of eddies as "catalysts" transferring mean momentum from one level to another. Similar analysis can be performed in a full three-dimensional case and for the thermodynamic equation as well. The result is a set of equations for the zonal-mean variables that are "forced" by the eddy fluxes of momentum and heat.

Linearized Zonal-Mean Model

We will discuss here what is perhaps the simplest useful model for the mean circulation in the middle atmosphere. In particular, we consider the steady-state response of the mean flow to a specified eddy forcing. The model has the realistic feature that diabatic effects act to restore radiative equilibrium. For simplicity we will model this radiative effect with a Newtonian cooling towards a state with

no meridional temperature gradient (it is easy to generalize to the case where the "radiative equilibrium" state has a meridional gradient). Also, for mathematical tractability, we will consider only the Boussinesq equations on an f-plane (periodic boundary conditions in the x-direction will represent the zonal periodicity of the real atmosphere). The base state static stability is assumed constant and some non-linear advection terms are ignored. With all these assumptions the governing equations for the zonally-averaged circulation reduce to:

$$-f\bar{v} = \bar{F}_{eddy}$$

$$f\bar{u} = -\frac{1}{\rho_0}\frac{\partial \bar{P}'}{\partial y}$$

$$\frac{\partial \bar{P}'}{\partial z} = -g\bar{\rho}'$$

$$\bar{w}\bar{\rho}_z = -\alpha\bar{\rho}'$$

$$\frac{\partial \bar{v}}{\partial y} + \frac{\partial \bar{w}}{\partial z} = 0$$

where

$$\bar{\rho} = \rho_0 + z\bar{\rho}_z + \bar{\rho}'$$

and

$$\bar{P} = \bar{P}_0 + \bar{P}'$$

Note that we have ignored the eddy terms in the thermodynamic equation for simplicity. [For those familiar with the Transformed Eulerian Mean (TEM)

formulation (e.g., Andrews et al., 1987) another approach is to take these same equations and replace $\overline{w}$ and $\overline{v}$ with the TEM velocities $\overline{w^*}$ and $\overline{v^*}$ - this accounts for the effects of the eddy heat transports in a consistent way.]

The thermodynamic equation can be rewritten as

$$N^2\bar{w} = \frac{\alpha g}{\rho_0}\bar{\rho}'$$

where

$$N^2 = -\frac{g\bar{\rho}_z}{\rho_0}$$

Here, f is the Coriolis parameter (a constant), $\bar{u}$ is the zonally-averaged zonal velocity, $\bar{v}$ and $\bar{w}$ are the meridional and vertical components of the mean meridional circulation, N is the buoyancy frequency, $\bar{P}$ is the zonal-mean pressure and $\bar{\rho}$ is the zonal-mean density. The density is the sum of a background state and the perturbation $\bar{\rho}'$. The background state density is the sum of the constant Boussinesq mean density, $\bar{\rho}_0$, and a linear decrease with height. The background pressure $\bar{P}_0$ is assumed to be in hydrostatic balance with the background density. The body force per unit mass associated with the eddy Reynolds stress convergence [or Eliassen-Palm flux divergence in the TEM case] is $\bar{F}_{eddy}$, and the Newtonian cooling has a relaxation coefficient α.

These linear, constant coefficient equations are easily solved if we write the solution in terms of Fourier harmonics. Consider one harmonic:

$$\bar{F}_{eddy}, \bar{P}', \bar{\rho}', \bar{u}, \bar{v}, \bar{w} \propto e^{i(ky+mz)}$$

Substitution into the equations of motion gives

$$\bar{v} = -\frac{\bar{F}_{eddy}}{f} \tag{1}$$

$$f\bar{u} = -\frac{ik\bar{P}}{\rho_0} \tag{2}$$

$$im\bar{P} = -g\bar{\rho}' \tag{3}$$

$$\frac{\rho_0 N^2 \bar{w}}{\alpha} = g\bar{\rho}' \tag{4}$$

$$ik\bar{v} + im\bar{w} = 0 \tag{5}$$

Equations (3) and (4) can be combined to give

$$\frac{\rho_0 N^2 \bar{w}}{\alpha} = -im\bar{P}$$

or

$$im\bar{w} = \frac{\alpha}{\rho_0 N^2} m^2 \bar{P}$$

Substituting this into (5) and using (1) to eliminate $\bar{w}$ and $\bar{v}$ gives

$$-ik\frac{\bar{F}_{eddy}}{f} + \frac{\alpha m^2}{\rho_0 N^2}\bar{P} = 0$$

or

$$\bar{P} = \frac{ik\rho_0 N^2}{f\alpha m^2}\bar{F}_{eddy}$$

From equation (2) then

$$\bar{u} = -\frac{ik}{f\rho_0}\bar{P} = \frac{k^2 N^2}{f^2 m^2 \alpha}\bar{F}_{eddy} \tag{6}$$

The response of $\bar{u}$ to the forcing is proportional to $1/f^2$, which implies that, for given spatial scales of the forcing, the constraint of the "radiative spring" on the mean flow is very much less effective near the equator than at higher latitudes. One factor of $1/f$ arises because the temperature perturbation associated with a given wind perturbation scales as f, and there is an additional factor of $1/f$ because the induced meridional circulation affects the zonal momentum equation through the $f\bar{v}$ term.

Since m^2 in equation (6) is equivalent to a second derivative in z on the zonal velocity, this acts as a vertical diffusion, i.e.

$$\frac{\partial^2 \bar{u}}{\partial z^2} = -\frac{k^2 N^2}{f^2 \alpha} \bar{F}_{eddy}$$

or in general, with a non-resting background state,

$$\frac{\partial^2 (\bar{u} - \bar{u}_{rad})}{\partial z^2} = -\frac{k^2 N^2}{f^2 \alpha} \bar{F}_{eddy}$$

where $\bar{u}_{rad}$ is the zonal mean wind that is in thermal wind balance with the radiative equilibrium temperature structure. The radiative spring acts as an "effective vertical diffusion" diffusing away any deviations from the radiative equilibrium state.

This process has a characteristic time-scale $\bar{u}/F_{eddy}$ or $\frac{k^2 N^2}{f^2 m^2 \alpha}$. At sufficiently small f this will become very long, and it is unlikely that the steady-state solution has much relevance. Near the equator the dominant balance is presumably between $\partial \bar{u}/\partial t$ and $\bar{F}_{eddy}$. Thus at low latitudes the mean flow can respond to eddy driving with sustained accelerations. The momentum in the zonal-mean flow at any time has responded to the accumulated effect of the eddy driving and serves as a "memory" for the atmospheric circulation.

This treatment of the mean flow effects in the tropical middle atmosphere has been highly idealized, of course. Some aspects involved in more realistic models are discussed by Dunkerton (1991). For example, Dunkerton notes that in a compressible atmosphere the effective diffusion does not act symmetrically in the upward and downward directions as it does in the simple Boussinesq case considered here. The work of Haynes et al. (1991) is also relevant. This is a more general discussion of the response of the zonal-mean circulation to imposed forces, including such aspects as the nonlinear advection of the relative mean momentum by the mean meridional circulation, and the spherical geometry. Their results also demonstrate

the difficulty in finding a steady-state mean flow response at low latitudes that would be relevant to the real atmosphere.

3. Phenomenology of Tropical Circulation

3.1 Historical Introduction

The first scientific knowledge of the winds in the tropical stratosphere was obtained from observations of the motion of the aerosol cloud produced by the eruption of Mt. Krakatoa (modern-day Indonesia) in August 1883. The optical phenomena caused by the aerosol were remarkable enough that their first appearance was widely noted. The UK Royal Society collected observations from over 30 locations in the tropics and plotted the motion of the edge of the aerosol cloud (see Fig. 10). The regular westward motion is evident, and these observations imply a mean easterly wind velocity between about 31 and 34 m-s^{-1}.

The wind in the tropical lower stratosphere was first measured with pilot balloons in 1908 by von Berson at two locations in equatorial East Africa. Over the next three decades these observations were followed by sporadic measurements at a number of tropical locations (see Hamilton, 1998, for a review of these early observations). The results sometimes indicated easterly winds and sometimes westerly winds, a state of affairs reconciled at the time by assuming that there was a narrow ribbon of westerlies (the "Berson westerlies") embedded in the prevailing easterly current revealed by the Krakatoa observations (e.g., Palmer, 1954).

Regular balloon observations of the lower stratospheric winds in the tropics began at a number of stations in the early 1950's. By the end of the decade it was obvious that both the easterly and westerly regimes at any height covered the entire equatorial region, but that easterlies and westerlies alternated with a roughly biennial period (Veryard and Ebdon, 1961; Reed et al., 1961). Initially it was thought that the period of the oscillation might be exactly two years, but as measurements accumulated it soon became clear that the period of oscillation

was somewhat irregular and averaged over 2 years. By the mid-1960s the term "quasi-biennial oscillation" (QBO) had been coined to denote this puzzling aspect of the stratospheric circulation.

3.2 Modern Observations of the QBO

Height-Time Dependence at Low latitudes

Much of what we know about the QBO has come from analysis of operational balloon-borne radiosonde observations, although such observations are generally restricted to a ceiling near 10 hPa ($\sim$30 km) and the number of near-equatorial stations is relatively limited. Fig. 11 shows an 8-year time series of monthly-mean 30 mb zonal wind computed simply by averaging twice-daily balloon observations at Singapore (1.4N). This illustrates many of the key features of the QBO. Note that the time series is clearly dominated by an alternation between easterly and westerly wind regimes roughly every other year. The extremes in the prevailing winds vary somewhat from cycle to cycle, but the peak easterly (in the monthly mean) usually exceeds 30 m-s^{-1}, while the westerly extreme is usually between 10 and 20 m-s^{-1}. The time series has a rough square-wave character with rapid transitions ($\sim$2-4 months) between periods of fairly constant prevailing easterlies or westerlies.

A hand-drawn height-time contour plot of the monthly-mean zonal wind from 100 hPa ($\sim$17 km) and 10 hPa ($\sim$30 km) for four years at Canton Island (2.8N) is shown in Fig. 12. This shows that the wind reversals appear first at high levels and then descend. At any level the transition between easterly and westerly regimes is rapid, so that the transitions are also associated with strong vertical shear.

The height-time evolution of the monthly-mean wind near the equator for over four decades is shown in Fig. 13 (an updated version of the figure published in

16

Naujokat, 1986) Unfortunately there has not been a single, continuously-operating, near-equatorial station taking appropriate observations over this period. This results shown in Fig. 13 were spliced together from records at Canton Is. (2.8N), Gan (0.7S) and Singapore (1.4N). These near-equatorial data suggest that the mean period of the oscillation is close to 28 months and varies between about 20 months and 36 months. Much of the variability in period is associated with the changes in the length of the easterly phase at and above about 30 hPa and in the westerly phase at and below about 50 hPa. The maximum amplitude occurs near 30 mb and the amplitude drops off to small, but apparently still detectable, values near the tropopause ($\sim$17 km). The dropoff in QBO amplitude above 30 mb is very gradual and the oscillation is still very strong at the 10 mb level. At almost all levels and all times the easterly-to-westerly transitions are more rapid than *vice versa*, and the associated westerly shear zones are considerably more intense than the easterly shear zones.

There is only a very limited network of radiosonde stations near the equator regularly reporting stratospheric winds. An assumption implicit in most observational studies is that the prevailing winds near the equator are essentially zonally-symmetric. Belmont and Dartt (1968) tried to check this with available radiosonde data and concluded that the QBO was indeed very nearly zonally-symmetric up to 50 hPa (above this level they felt they had inadequate data to verify this). Recently the advent of Doppler-radiometer observations of horizontal winds by the High Resolution Doppler Imager (HRDI) instrument on the Upper Atmosphere Research Satellite (e.g., Ortland et al., 1996) has provided another opportunity to examine this issue. Ortland (1997) finds that there may be some modest ($\sim$10 m-s^{-1}) zonal asymmetries in the monthly-mean wind at the equator in the westerly phase of the QBO, particularly at and above 10 mb. This issue will be discussed

further below, but, to first order, the assumption of a zonally-symmetric QBO is appropriate.

The vertical structure of the equatorial QBO above the operational balloon ceiling was initially studied by rocket-borne sondes. Fig. 14 shows the zonal wind observations from actual individual rocket soundings for 25 months at Ascension Island (8S). Results at 28 km show an obvious QBO signal, but at higher altitudes the QBO amplitude clearly drops off while the semiannual (6-month) variation dominates by 48 km. Fig. 15 shows a long height-time series of monthly-mean zonal wind near the equator constructed by using the balloon observations at Canton Is., Gan and Singapore below 31 km, and an average of rocketsonde observations at Kwajalein (9N) and Ascension Is. (8S) above 31 km. The top panel shows the deseasonalized values, while the bottom panel shows a band-passed version including only periods between 9 and 48 months. The filtering in both cases eliminates the mean semiannual variation, allowing the QBO to stand out. The drop off of the QBO amplitude in the upper stratosphere is evident.

The advent of the HRDI satellite observations has allowed the structure of the wind QBO at still higher levels to be investigated. The top panel of Fig. 16 shows the height-time section of equatorial zonal-mean winds estimated from the HRDI observations from Jan. 1992-July 1997 and from 10-100 km (with a gap near 45 km). The bottom panel shows the same section, but with the annual and semiannual harmonics removed, emphasizing the interannual variations. The QBO in the lower-middle stratosphere evident. Also apparent is a less smooth interannual variation peaking around 85 km. The vertical wiggly lines emphasize the apparent connection of the variations near 85 km with those in the lower stratosphere. Whenever there are easterly (westerly) anomalies through a thick layer in the lower stratosphere, strong westerly (easterly) anomalies appear near

the mesopause. The high level variations are often referred to as the "mesopause QBO (MQBO)".

Meridional Modulation

While the QBO in zonal-wind has little longitudinal structure, it does have a very strong dependence on latitude. Fig. 17, taken from Dunkerton and Delisi (1985), shows the evolution of 30 hPa zonal winds during 1964-1983 determined for various latitudes by averaging balloon observations at clusters of stations located near the indicated latitude. So, for example, the results shown for the equator are actually averages over Singapore (1.4N), Gan (0.7S) and Nairobi (1.3N), and those labelled "19N" are averages over Hilo (19.7N), Wake (19.3N) and Grand Cayman (19.3N). The strongly near-equatorial character of the QBO is evident from even a cursory inspection of these data. Near the equator the data show almost nothing but the QBO, by 19 or 20 degrees latitude the QBO is hardly apparent, and is swamped by the seasonal cycle.

Fig. 18 shows a determination of the amplitude (solid contours) and phase (dashed contours) of the QBO in zonal wind as a function of height and latitude in the tropical stratosphere. It was derived by R.J. Reed who performed a least-squares fit of a single 26-month harmonic to about 8 years of balloonsonde zonal wind data at a number of low latitude stations (see Wallace, 1973). Unlike purely periodic phenomena the determination of amplitude and phase for the QBO is not straightforward. Other studies have followed Reed in fitting a fixed-period harmonic to the data. Such a procedure will not provide stable results - amplitudes will drop the longer the record analyzed, so Reed's application to a relatively brief record may be essentially optimal. Fig. 18 shows that the amplitude has a peak centered squarely on the equator and a roughly Gaussian dropoff in latitude with an *e*-folding width of between 13 and 15 degrees of latitude. The phase lines

19

are remarkably regular indicating a steady downward propagation of about 2 km-month^{-1} and very little phase variation in latitude.

The single harmonic approach obscures some of the characteristic details of the meridional evolution of the zonal wind through the QBO cycle. In particular, the initial westerly accelerations away from the easterly extreme tend to be very narrowly-confined near the equator, and then the "westerly tongue" expands so that the extreme westerly jet is of about the same width as the easterly jet. This is illustrated in Fig. 19 (from Hamilton, 1987) that shows the zonal wind at 30 hPa month-by-month from October 1979 through February 1980.

Reed's analysis shows the amplitude of the QBO dropping to near zero at 25 degrees latitude. Later on we will discuss the influence of the QBO at higher latitudes.

QBO in Temperature

A QBO in temperature has also been clearly observed. The bottom curve in Fig. 20 shows the temperature anomalies (deviations from long-term climatology) averaged over the 30-50 hPa layer based on Singapore balloon observations. A QBO with peak-to-peak amplitude of around 8°C is evident. The top curve shows the vertical shear in the zonal wind over the 30-50 hPa layer, again from the Singapore balloon observations. The strong positive correlation between the two time series is clear, and can be explained in terms of the thermal wind balance discussed earlier. In general, the usefulness of the geostrophic approximation breaks down at low latitudes, of course, but in fact the *zonal-mean* component of the circulation should be close to geostrophic balance.

Period Modulation of the QBO

When a long record of QBO winds is examined, some order appears in the

20

variability from cycle-to-cycle. The QBO amplitude appears to be fairly constant, but the period length varies significantly with time. This variability has some very characteristic features. Below about 30 hPa the easterly phases are of nearly constant length, but the westerly phases vary by a factor of two. Fig. 21 shows a determination of the length of the westerly phases at 45 hPa through 4 decades. As noted by Salby and Callaghan (2000) the period seems to vary systematically with a quasi-decadal time scale. Salby and Callaghan speculated that the 11-year solar cycle may be somehow controlling the QBO period. Later on we will consider other possible explanations for the variability of QBO period.

Above about 30 hPa, the situation reverses: the westerly phases are of roughly comparable length, but the easterly phases are quite variable.

Another interesting aspect of the QBO is the subtle effect of the annual cycle. As noted earlier, the long-term mean period of the QBO is incommensurate with the annual period or any obvious harmonic or subharmonic. However, the annual cycle does have some statistical connection with the observed QBO-related wind transitions. Fig. 22 is a histogram of the month-of-year in which the 50 hPa westerly-to-easterly and easterly-to-westerly zero crossings were observed. There is a strong concentration of such transitions in the May-July period of the year. Again this subtle connection with the annual cycle is something that needs to be explained dynamically.

3.3 Observations of the Semiannual Oscillation

The first knowledge of the wind field above the ceiling for balloon observations was obtained with rocket soundings. Fig. 14 shows all the zonal wind observations from rocket soundings during a two year period at Ascension Is. (8°S). In the middle stratosphere the QBO appears quite clearly (at least to $\sim$ 40 km) However,

21

at upper stratospheric levels the QBO is dominated by a shorter period oscillation. We now know that this is a semiannual oscillation (SAO). Unlike the QBO, the SAO is very clearly phase-locked to the calendar. Near the stratopause the easterly extremes are reached in January and July and the westerly extremes around April and October. Fig. 23 shows a climatological annual march of the zonal wind deduced from rocket observations at a number of sites. At the equator the semiannual variation clearly dominates in a thick layer around the stratopause. The vertical structure of the westerly accelerations displays a downward propagation that is similar to the QBO wind reversals. The easterly accelerations are more uniform in height. The stratopause SAO has been seen in rocket observations of zonal winds, rocket observations of temperatures (e.g., Garcia et al., 1997; Dunkerton and Delisi, 1997), satellite radiometer measurements of temperature (Hitchman and Leovy, 1986; Delisi and Dunkerton, 1988) and the recent HRDI Doppler radiometer measurements of winds (Burrage et al., 1996).

Fig. 24 shows the height-latitude structure of the amplitude of the semiannual component of the zonal wind variation determined from rocketsonde observations at several stations. Like the QBO, the SAO appears to have a similar equatorially-trapped structure. This is shown as well in Fig. 25 which displays the height-latitude structure of the amplitude of the semiannual component of zonal-mean temperature determined from satellite radiometer observations.

Using the limited number of rocket soundings available at very high altitudes, Hirota (1978) and Hamilton (1982a) were able to show that the amplitude of the SAO at low latitudes drops in the lower mesosphere, but rises again to a maximum near the mesopause. They also found that the SAO at the mesopause is nearly 180° out of phase with the stratopause SAO. Fig. 26 shows Hirota's hand-contoured plot of the zonal wind measured at Ascension Is. each month from 1970-1972. In

each month data up to the usual meteorological rocketsonde ceiling (∼60 km) are available, and in about 18 months there are some data from special rockets that go up to 90 km. The long-term mean and annual cycle at each height have been removed. This figure shows the stratopause SAO centered around 50 km, and also a second maximum in SAO amplitude around 80-85 km. This "mesopause SAO" is nearly 180 degrees out-of-phase with the stratopause SAO.

These early rocket observations of the mesopause SAO have been confirmed recently with the wind measurements from the HRDI instrument. This can be seen in the raw HRDI timeseries in the top panel of Fig. 16. Fig. 27 (from Garcia et al., 1997) shows the equatorial zonally-averaged zonal wind as a function of height and time of year composited from the HRDI measurements in the height range 65-110 km. The prominent SAO at the mesopause seen in these data has amplitude comparable to that observed near the stratopause.

3.4 Observations of High-Frequency Waves in the Tropical Atmosphere

The discussion thus far has focussed on analysis of monthly-mean observations. In addition to the slow variations that are revealed in the monthly-means, the tropical stratosphere and mesosphere display significant day-to-day and hour-to-hour variations. The top panel in Fig 28 shows the height-time section of zonal wind at Balboa (9N) for 6 months plotted using daily balloon data, while the bottom panel shows the same thing, but for temperature observations. The overall descending QBO phases are evident in each of these sections. However, just as prominent are oscillations of periods appearing to be ∼2-20 days. These variations also display a predominant downward phase progression. As we will see, these higher frequency waves are thought to be essentially internal gravity waves, modified by the effects

of the earth's rotation. In this interpretation, the downward phase propagation corresponds to upward wave energy (or, more exactly, wave activity) propagation, suggesting a dominant tropospheric source for the waves.

Similar waves are observed higher up as well. Fig. 29 (from Hirota, 1978) shows the difference in u and T between two rocket soundings at Ascension Is. separated by two days. There are wiggles at various scales apparent, but most prominent is a variation with vertical wavelength of about 20 km which looks very coherent between the zonal wind and temperature.

The wave activity in the low-latitude stratosphere is observed to be significantly modulated by the QBO. The contours in Fig. 30 shows the time power spectra of u and T variations calculated from twice-daily balloon observations over the 20-25 km layer at Singapore plotted each month for several years. Also shown as the heavy line is the time series of monthly-mean zonal wind. The spectra show maxima around periods of 10 days, but these peaks become much more prominent near the easterly extreme of the QBO. As we shall see, the coupling of the high frequency waves with the mean flow is thought to be crucial for the generation of the QBO.

Balloon and rocket observations are usually taken at most twice-pre-day. Other kinds of observations such as radars and lidars show that significant wave variations in the middle atmosphere occur at even higher frequencies.

There is considerable data concerning the height-time variations of middle atmospheric wind and temperature at single stations. Rarer is useful information on the horizontal structure of the wave variations, and even rarer are observations that reveal the time-horizontal structure of middle atmospheric variations. At fairly low frequency (say many days to weeks) there is some indication of fairly coherent, long

24

zonal scale structures. Some of the early studies of waves in the tropical strato-
sphere focussed on planetary-scale waves that can be examined by using the daily
balloon observations from widely separated radiosonde stations (see Wallace, 1973,
for a review of this early work). It is now fairly clear that such coherent, planetary-
scale waves are only a part of the full spectrum of waves in the middle atmosphere.
Aircraft observations suggest that there is a rather shallow continuous spectrum
of horizontal variations out to scales as small as 10 km. Fig. 31 shows mean
horizontal power spectra in the upper troposphere calculated from observations
from thousands of instrumented commercial aircraft. One key unresolved question
that will arise in various contexts in these lectures is the relative importance of
relatively small-scale gravity waves and the lower-frequency planetary-scale waves
in the general circulation of the tropical middle atmosphere. Unfortunately, the
currently available observations do not provide definitive information about this
issue.

4. Simple Model of Wave-Driving of the Mean Flow

4.1 Introduction

The considerations outlined in Section 2 above explain the propensity of the zonal-mean tropical middle atmospheric circulation to undergo slow variations. The basic explanation for why the variations can take the form of the quasi-regular QBO wind reversals was provided by Lindzen and Holton (1968) and Holton and Lindzen (1972). They showed that the eddy driving of the mean flow from a combination of eastward and westward travelling, vertically-propagating, internal gravity waves or equatorial planetary waves could produce a long-period mean flow oscillation with many of the observed characteristics of the QBO. This section will discuss simple models that demonstrate how waves interacting with the mean flow may give rise to the long-period QBO phenomenon. later lectures will discuss related issues such as the details of the wave dynamics in the equatorial region (in particular the role of planetary rotation), and the tropospheric forcing mechanisms for these waves.

Plumb (1977) presented a slightly simplified version of the Holton-Lindzen model which simply considers the mean flow accelerations induced by two internal gravity waves. We will describe the Plumb model in some detail here. The first step will be a brief discussion of the properties of linear internal gravity waves.

4.2 Two-Dimensional Internal Gravity Waves

We consider the case of purely 2-D, non-rotating flow in a domain with periodic boundary conditions in the x-direction. For simplicity we will treat the problem within the Boussinesq and hydrostatic approximations. Consider then the equa-

tions linearized about a time-independent, zonal-mean state characterized by mean flow $\bar{u}(z)$, and mean static stability $N(z)$.

$$\frac{\partial u'}{\partial t} + \bar{u}\frac{\partial u'}{\partial x} + w'\frac{\partial \bar{u}}{\partial z} = -\frac{1}{\rho_0}\frac{\partial P'}{\partial x} - \alpha u' \tag{7}$$

$$\frac{\partial \rho'}{\partial t} + \bar{u}\frac{\partial \rho'}{\partial x} - \frac{\rho_0 N^2}{g}w' = -\alpha \rho' \tag{8}$$

$$\frac{\partial P'}{\partial z} = -g\rho' \tag{9}$$

$$\frac{\partial u'}{\partial x} + \frac{\partial w'}{\partial z} = 0 \tag{10}$$

Where we have allowed for the possibility of wave dissipation by inclusion of the linear relaxations in the momentum and thermodynamic equations. Now assume travelling wave solutions

$$u' = U(z)e^{i(kx-\omega t)}$$

$$w' = W(z)e^{i(kx-\omega t)}$$

etc.

Substitution into equations (7)-(10), and assuming that $\alpha = 0$, gives

$$\frac{\partial^2 W}{\partial z^2} + \left(\frac{N^2 k^2}{(\omega - k\bar{u})^2}\right)W + \left(\frac{k}{(\omega - k\bar{u})}\right)\frac{\partial^2 \bar{u}}{\partial^2 z}W = 0$$

If we now assume that the background state does not vary with height so that $N^2(z)$ and $\bar{u}(z)$ are constant, then

$$\frac{\partial^2 W}{\partial z^2} + \left(\frac{k}{\omega - k\bar{u}}\right)^2 N^2 W = 0 \tag{11}$$

The solution to this equation is of the form $W \propto e^{imz}$ and the resulting dispersion relation is

$$m^2 = \frac{N^2 k^2}{(\omega - \bar{u}k)^2} = \frac{N^2}{\hat{c}^2}$$

where $\hat{c}$ is the intrinsic (Doppler-shifted) horizontal phase speed for the wave. Waves with high intrinsic horizontal phase speed have small m, or long vertical wavelength. Also, near critical levels, where the horizontal phase speed matches the background flow, the vertical wavelength should become very small.

The vertical group velocity is given by

$$c_{g_z} = \frac{\partial \omega}{\partial m} = \frac{\partial (\omega - \bar{u}k)}{\partial m}$$

Using as our convention that the intrinsic frequency of the waves is positive, the appropriate root must be taken:

$$\omega - \bar{u}k = \pm \frac{Nk}{m}$$

where the sign of k and m determine the sense of phase propagation. This gives a vertical group velocity

$$c_{g_z} = \mp \frac{Nk}{m^2} = \mp \frac{(\omega - \bar{u}k)^2}{Nk}$$

This implies that for $m < 0$ (i.e. for waves with downward phase propagation), $c_{g_z} > 0$ and so there is upward group propagation. Also, higher intrinsic horizontal phase speed waves have larger vertical group velocity. As $\omega \to \bar{u}k$ the vertical group velocity $c_g \to 0$.

One can also easily show for $c_{g_z} > 0$, that $\overline{u'w'} > 0$, if $k > 0$, and that $\overline{u'w'} < 0$, if $k < 0$. That is, for upward-propagating wave energy with eastward (westward) intrinsic phase speed the eddy momentum flux is positive (negative).

For the general case when the mean state varies with height, the full equation for $W(z)$ is needed. However, if we assume that the mean state varies sufficiently slowly with height relative to the wave phase, i.e.

$$\frac{k}{|\omega - \bar{u}k|}\frac{\partial^2 \bar{u}}{\partial z^2} \ll m^2$$

then the dominant balance is just that described by equation (11). Again if $\bar{u}$ and N^2 vary only slowly with z over a vertical scale m^{-1}, then we can use the WKB solution

$$W(z) = W(z_0)\Big(\frac{kN}{\omega - \bar{u}k}\Big)^{1/2}exp\Big(\int_{z_0}^{z} -\frac{ikN}{\omega - \bar{u}k}dz\Big) \tag{12}$$

where we have considered a wave with upward group velocity. In this case, one can go back to the governing equations and - assuming a slowly-varying mean state - show that $\overline{u'w'}(z) = constant$, which is consistent with the Eliassen-Palm theorem (i.e. that for steady, unforced and undissipated linear gravity waves the divergence of the Reynolds stress should be zero; see Eliassen and Palm, 1961).

Including the dissipation terms $-\alpha u'$ and $-\alpha \rho'$, in the above derivation simply replaces ω by $\omega + i\alpha$. In this case, the integral in equation (12) becomes

$$\int_{z_0}^{z} -\frac{kN}{\omega + i\alpha - \bar{u}k}dz$$

$$= \int_{z_0}^{z} -\frac{ikN}{(\omega - \bar{u}k)(1 + \frac{i\alpha}{\omega - \bar{u}k})}dz$$

Assuming weak dissipation (i.e. that $\alpha \ll (\omega - \bar{u}k)$) and using a binomial expansion, the integral becomes

$$\approx \int_{z_0}^{z} \Big(-\frac{ikN}{(\omega - \bar{u}k)} + \frac{i^2 \alpha kN}{(\omega - \bar{u}k)^2}\Big)dz$$

$$= \int_{z_0}^{z} -\frac{ikN}{(\omega - \bar{u}k)}dz - \int_{z_0}^{z} \frac{\alpha kN}{(\omega - \bar{u}k)^2}dz$$

29

so that the solution has both an oscillating character and an overall amplitude modulation with an exponential decay with height. In this case, the Reynolds stress is no longer constant but

$$\overline{u'w'}(z) \sim exp\Big(\int_{z_0}^{z} -\frac{2\alpha k N}{(\omega - \bar{u}k)^2}dz\Big) = exp\Big(\int_{z_0}^{z} -\frac{2\alpha}{c_{g_z}}dz\Big)$$

Therefore, the slower the vertical group velocity, the longer the damping can act on the waves, the more rapid the decay of the Reynolds stress, and the stronger the local mean flow driving. Note that in general α can be a function of z. If the damping term is omitted from the momentum equation but retained in the thermodynamic equation, it is easy to show that

$$\overline{u'w'}(z) = \overline{u'w'}(z_0)exp\Big(\int_{z_0}^{z} -\frac{\alpha k N}{(\omega - \bar{u}k)^2}dz\Big). \tag{13}$$

This is the case considered by Plumb (1977) in his original paper, and it is possibly a reasonable treatment of the stratosphere in the sense that large-scale motions may be regarded as rather inviscid, while the effects of radiative transfer will definitely act to damp the temperature perturbations associated with wave motions. The effectiveness of radiative transfer in damping waves is known to depend on the vertical wavelength, with short wavelengths more strongly damped (e.g. Fels, 1982). In the limit of very long vertical wavelength perturbations the timescale for the radiative damping can be estimated to range from ~ 100 days in the lowermost stratosphere to ~ 5 days near the stratopause. Fig. 32 shows a typical profile used for the thermal damping rate in the stratosphere. The dissipation rates given in this figure are for long vertical wavelengths and thus are something of an underestimate of those appropriate for the waves (with wavelengths roughly 3-15 km) thought to be important in driving the mean flow accelerations in the tropical stratosphere (e.g. Wallace, 1973).

4.3 One-Wave Plumb model

Consider a system with a zonal-mean flow $\bar{u}(z, t)$ and one internal gravity wave, with wavenumber k and frequency ω, forced at the lower boundary. Assume that there is a constant effective vertical diffusion K acting on the mean flow. Then the zonal-mean zonal momentum equation is

$$\frac{\partial \bar{u}}{\partial t} = -\frac{\partial}{\partial z}(\overline{u'w'}) + K\frac{\partial^2 \bar{u}}{\partial z^2}$$

We follow the standard treatment of wave-mean flow interaction problems in assuming that the eddy fluxes can be adequately computed from linear wave theory. In addition we assume that the vertical wavelength of the wave is sufficiently short that the WKB scaling discussed earlier applies, and that the mean flow changes so slowly that the steady wave solution can be used. In this case we saw that the wave momentum flux is given by equation (13). In that equation z_0 is height of the lower boundary, which can be regarded as corresponding to the tropopause. All the wave parameters, including the momentum flux at z_0, must be specified, along with $N(z)$ and $\alpha(z)$. Using boundary conditions on the mean flow such that $\bar{u}(z_0) = 0$ and $\frac{\partial \bar{u}}{\partial z} = 0$ at the top boundary, one can integrate numerically very easily, calculating the wave flux, then using the flux convergence as forcing in the mean flow equation for some brief timestep, then recalculating the wave fluxes with the updated mean flow etc.

Fig. 33 shows the mean flow evolution in an integration of this model. The imposed gravity wave has a phase speed of $+30$ m-s^{-1} and a period of about 15 days. With an initial zonal wind $\bar{u}(t_0) = 0$, and with radiative damping that increases with height, the initial acceleration of the zonal wind is strongest higher up. As the wind is accelerated, however, the intrinsic phase speed of the wave decreases, leading to increased dissipation at lower levels. Eventually the wave is

almost choked off from reaching the upper levels and the accelerations there drop almost to zero. The net effect is to produce a mean flow jet with maximum that descends with time, very much like the wind regimes in the QBO. After 80 days the model is approaching a steady-state with the maximum mean flow comparable to the wave phase speed. At this point the wave is very strongly absorbed in the lowest few km of the domain and the eddy forcing is counteracted by the mean flow diffusion of momentum down into the lower boundary.

The model described here is easily generalized to include the effects of compressibility (e.g., Plumb, 1977). The WKB solution for the Reynolds stress associated with the vertically propagating gravity wave becomes

$$\rho_0(z)\overline{u'w'}(z) = \rho_0(z_0)\overline{u'w'}(z_0)exp\Big(\int_{z_0}^{z} -\frac{\alpha k N}{(\omega - \bar{u}k)^2}dz\Big).$$

where $\rho_0(z)$ is the mean density. The mean flow equation is generalized to

$$\frac{\partial \bar{u}}{\partial t} = -\frac{1}{\rho_0}\frac{\partial}{\partial z}(\rho_0\overline{u'w'}) + \frac{K}{\rho_0}\frac{\partial}{\partial z}(\rho_0\frac{\partial \bar{u}}{\partial z})$$

The reduction of mean density with height leads to more effective wave driving of the mean flow accelerations at higher levels. In the compressible model one can obtain a very pronounced downward progression of the jet maximum even with a wave dissipation rate, α, that is constant with height.

4.4 Two-Wave Plumb Model

The example above showed that the interaction of a single dissipating internal wave with the mean flow can produce monotonic mean flow accelerations that are

32

self-limiting. We now show that adding a second wave with phase speed in the opposite direction allows the mean flow to oscillate.

Consider a system with two waves such that $k_1 = -k_2$ and $\omega_1 = \omega_2$. The governing equation for the mean flow is now

$$\frac{\partial \bar{u}}{\partial t} = -\frac{\partial}{\partial z}(\overline{u'w'}) + K\frac{\partial^2 \bar{u}}{\partial z^2}$$

where the total Reynolds stress is

$$\overline{u'w'}(z) = \overline{u'w'}_1(z_0)exp\Big(\int_{z_0}^{z} -\frac{\alpha k_1 N}{(\omega_1 - \bar{u}k_1)^2}dz\Big) + \overline{u'w'}_2(z_0)exp\Big(\int_{z_0}^{z} -\frac{\alpha k_2 N}{(\omega_2 - \bar{u}k_2)^2}dz\Big)$$

For simplicity we suppose the waves have equal amplitudes at the lower boundary, so that

$$\overline{u'w'}_1(z_0) = -\overline{u'w'}_2(z_0)$$

Fig. 34 shows results from an integration of a 2-wave Plumb model using waves with phase speeds of +25 m/s and -25 m/s. The result shown is for a compressible version and other details can be found in Hamilton (1982b). The mean flow evolution displays an oscillation between positive and negative winds with a period of slightly over 1000 days, downward propagation of the wind reversals, and the development of intense shear zones. The basic resemblance to the observed QBO is striking and represents a nice demonstration that the downward propagation of the jets and shear zones can result purely from interactions with upward propagating waves, i.e. the basic forcing for the stratospheric QBO may be regarded as residing in the troposphere where the waves are excited.

The basic reason for the oscillatory behavior in Fig. 34 is easy to understand. Once the flow develops with strong winds in, say, the +x direction within the lower part of the domain, the propagation to upper levels of the wave with negative

phase speed is enhanced. When this wave is disspated at these upper levels a negative jet is formed. This is a kind of "shadowing effect" in which the effects of a spectrum of vertically-propagating waves tends to produce a mean flow anomaly aloft of opposite sign to that at lower levels. The negative jet produced aloft can descend just as in the 1-wave case. Once the negative jet has descended low enough the effects of the mean flow viscosity destroy the positive jet below, allowing the negative mean flow region to descend right to the lower boundary. The process can then continue with a positive jet produced aloft, and so on. This process is illustrated schematically in Fig. 35.

The behaviour of the simple 2-wave Plumb model described here has been reproduced in a laboratory experiment by Plumb and McEwan (1978). They put salt-stratified water into an annulus with a flexible membrane at the bottom. The membrane was then forced up and down in order to excite a standing oscillation at the bottom. Since the standing oscillation can be regarded as the sum of two waves with equal but opposite phase velocities, the laboratory experiment is almost a direct analogue of the 2-wave Plumb model (with the annulus geometry supplying the periodic boundary conditions). The results were quite dramatic, as the waves produced a much longer period oscillation in the annulus-averaged circulation with downward-propagating flow reversals.

4.5 Further Development of Simple QBO Models

Perhaps the most fundamental problem impeding our understanding of the dynamics of the QBO is the inability to diagnose accurately from observations the actual contributions of different parts of the wave spectrum to the mean flow accelerations in the tropics. A direct calculation of the vertical Reynolds stress requires knowledge of the vertical wind, which cannot be directly measured on a

regular basis. Even the planetary-scale variations of the horizontal wind in the tropical stratosphere are hard to determine, given the sparse radiosonde network and the difficulty in obtaining reliable estimates of the wind from satellite temperature observations. This lack of a firm observational quantitative understanding affected the development of QBO theory from the beginning. In fact, the original model of Lindzen and Holton (1968) supposed that the forcing of the mean flow was due to gravity waves with a continuous spectrum of horizontal phase speeds, while the same authors four years later (Holton and Lindzen, 1972) showed that similar results could be obtained by including only one eastward-propagating and one westward-propagating large-scale equatorial planetary wave. Even today we cannot be certain of the relative contributions of planetary-scale waves and smaller-scale gravity waves.

The 1972 Holton and Lindzen paper presents a theory very similar to that of Plumb (1977), except that the expressions for vertical group velocity of the equatorial Kelvin and Rossby-gravity waves are used for the eastward and the westward-propagating waves, respectively (see Lindzen, 1971). The choice of wave parameters in the model was roughly based on available observations of planetary-scale equatorial waves (see Wallace, 1973, for a review). The results were quite encouraging, since with "reasonable" parameters the model was found to simulate an equatorial QBO with roughly the correct period, amplitude and vertical structure.

Much of the theoretical work on the QBO over the last 25 years has involved generalizations of the Holton-Lindzen (1972) model. Dunkerton (1981) considered the effects of wave transience in the model (i.e. he relaxed the assumption of steadiness in the calculation of the wave fluxes). Saravanan (1990) generalized the Holton-Lindzen model to include a large number of waves. Dunkerton (1983) added

an additional easterly forcing to the Holton-Lindzen model which was meant to account for the effects of mean flow forcing from quasi-stationary planetary waves forced by topography in the extratropics.

A major limitation of the Holton-Lindzen and Plumb QBO models is their restriction to one spatial dimension, i.e. they solve for the height and time dependence of a mean flow meant to represent the flow averaged over some latitude band around the equator. Plumb and Bell (1982) constructed a numerical model of the QBO forced by two waves, but including a treatment of the waves and mean flow in both height and latitude. Also included in the Plumb and Bell work was the effect of the vertical advection by the mean meridional circulation produced by mean flow radiative effects. They noted that the presence of westerly shear on the equator is associated with a warm anomaly at the equator and hence anomalous diabatic cooling, leading to mean sinking (or at least anomalously weak rising motion). This aspect of the QBO had been qualitatively discussed earlier by Reed (1965), and Reed's schematic diagram of this effect is reproduced here as Fig. 36. Plumb and Bell noted that the vertical advection associated with this component of the mean meridional circulation should act to intensify the accelerations as westerly jets descend, since the downward advection of the westerly momentum from above adds to the local westerly wave-driving. Conversely, the mean advection effect should act to weaken the easterly accelerations. Plumb and Bell proposed this as the mechanism to explain the observed asymmetry between the strengths of the easterly and westerly shear zones in the QBO.

Recently the possibility that a broad spectrum of gravity waves might be responsible for driving the QBO has been revived (e.g., Dunkerton, 1997). In one interesting development, Alexander and Holton (1997) conducted high-resolution limited-area explicit numerical simulations of a tropical squall line and found that

36

the momentum fluxes associated with the gravity waves forced by such storms could well be significant for the dynamics of the QBO.

References

Alexander, M.J. and J.R. Holton, 1997: A model study of zonal forcing in the equatorial stratosphere by convectively induced gravity waves. *J. Atmos. Sci., 54,* 408-419.

Andrews, D.G., J.R..Holton and C.B. Leovy, 1987: *Middle Atmosphere Dynamics*, Academic Press.

Baldwin, M., L. Gray, T. Dunkerton, K. Hamilton, P. Haynes, W. Randel, J. Holton, M. Alexander, I Hirota, T. Horinouchi, D. Jones, J. Kinnersley, C. Marquardt, K. Sato and M. Takahashi, 2001: The quasi-biennial oscillation. *Rev. Geophys., 39,* 179-229.

Belmont, A.D., and D.G. Dartt: 1968: Variation with longitude of the quasi-biennial oscillation. *Mon. Weath. Rev., 96,* 767-777.

Belmont, A.D., D.G. Dartt and G.D. Nastrom, 1974: Periodic variations in stratospheric zonal wind from 20 to 65 km at 80ºN to 70ºS. *Quart. J. Roy. Meteorol. Soc., 100,* 203-211.

Burrage, M.D. and coauthors, 1996: Long term variability in the equatorial mesosphere and lower thermosphere zonal winds. *J. Geophys. Res., 101,* 12847-12854.

Delisi, D. and T.J. Dunkerton, 1988: Equatorial semiannual oscillation in zonally averaged temperature observed by Nimbus-7 SAMS and LIMS. *J. Geophys. Res., 93,* 3899-3904.

Dunkerton, T.J., 1981: Wave transience in a compressible atmosphere, Pt. 2, Transient equatorial waves in the quasi-biennial oscillation. *J. Atmos. Sci., 38,* 298-307.

Dunkerton, T.J., 1983: Laterally-propagating Rossby waves in the easterly acceleration phase of the quasi-biennial oscillation. *Atmosphere-Ocean, 21,* 55-68.

Dunkerton, T.J., 1991: Nonlinear propagation of zonal winds in an atmosphere with Newtonian cooling. *J. Atmos. Sci., 48,* 236-263.

Dunkerton, T.J., 1997: The role of gravity waves in the quasi-biennial oscillations. *J. Geophys. Res., 102,* 26053-26076.

Dunkerton, T.J. and D. Delisi, 1985: Climatology of the equatorial lower stratosphere. *J. Atmos. Sci., 42,* 1199-1208.

Dunkerton, T.J. and D. Delisi, 1997: Interaction of the quasibiennial oscillation and the stratopause semiannual oscillation. *J. Geophys. Res., 102,* 26107-26116.

Eliassen, A. and E. Palm, 1961: On the transfer of energy in stationary mountain waves. *Geofys. Publ., 22,* 1-23.

Fels, S.B., 1982: A parameterization of scale-dependent radiative damping rates in the middle atmosphere. *J. Atmos. Sci., 39,* 1141-1152.

Forbes, J., 1981: The equatorial electrojet. *Rev. Geophys., 19,* 469-504.

Garcia, R.R., T.J. Dunkerton, R.S. Liebermann and R.A. Vincent, 1997: Climatology of the semiannual oscillation of the tropical middle atmosphere. *J. Geophys. Res., 102,* 26019-26032.

Hamilton, K., 1982a: Rocketsonde observations of the mesospheric semiannual oscillation at Kwajalein *Atmosphere-Ocean, 20,* 281-286.

Hamilton, K., 1982b: A note on the interaction between a Thermally Forced Standing Internal Gravity Wave and the Mean Flow: Implications for the Theory of the Quasi-biennial Oscillation. *J. Atmos. Sci., 39,* 1881-1886.

Hamilton, K., 1984: Mean wind evolution through the quasi-biennial cycle in the tropical lower stratosphere. *J. Atmos. Sci., 41,* 2113-2125.

Hamilton, K., 1985: The initial westerly acceleration phase of the stratospheric quasi-biennial oscillation as revealed in FGGE analyses. *Atmosphere-Ocean, 23,* 188-192.

Hamilton, K., 1987: A review of observations of the quasi-biennial and semi-annual oscillations of the tropical middle atmosphere. *Transport Processes in the Middle Atmosphere*, D. Riedel Publishing Co., pp. 19-29.

Hamilton, K., 1998: Observations of tropical stratospheric winds before World War II. *Bull. Amer. Meteorol. Soc., 79,* 1367-1371.

Haynes, P.H., C.J. Marks, M.E. McIntyre, T.G. Shepherd and K. Shine, 1991: On the downward control of extratropical diabatic circulations by eddy-induced mean zonal forces. *J. Atmos. Sci., 48,* 651-678.

Hirota, I., 1978: Equatorial Kelvin waves in the upper stratosphere in relation to the semiannual oscillation of the zonal wind. *J. Atmos. Sci., 35,* 714-722.

Hitchman, M.H. and C.B. Leovy, 1986: Evolution of the zonal mean state in the equatorial middle atmosphere during October 1978-May 1979. *J. Atmos. Sci., 43,* 3159-3176.

Holton, J.R. and R.S. Lindzen, 1972: An updated theory for the quasi-biennial cycle of the tropical stratosphere. *J. Atmos. Sci., 29,* 1076-1080.

Lindzen, R.S., 1971: Equatorial planetary waves in shear. Part I. *J. Atmos. Sci., 28,* 1452-1463.

Lindzen, R.S. and J.R. Holton, 1968: A theory of the quasi-biennial oscillation. *J. Atmos. Sci., 25,* 1095-1107.

Naujokat, B., 1986: An update of the observed quasi-biennial oscillation of the stratospheric winds over the tropics. *J. Atmos. Sci., 43,* 1873-1877.

Ortland, D.A. and coauthors, 1996: Measurements of stratospheric winds by the high resolution Doppler imager. *J. Geophys. Res., 101,* 10351-10363.

Palmer, C.E., 1954: The general circulation between 200 mb and 10 mb over the equatorial Pacific. *Weather, 9,* 3541-3549.

Plumb, R.A., 1977: The interaction of two internal waves with the mean flow: implications for the theory of the quasi-biennial oscillation. *J. Atmos. Sci., 34,* 1847-1858.

Plumb, R.A., 1984: The quasi-biennial oscillation. *Dynamics of the Middle Atmosphere* (J.R. Holton and T. Matsuno, eds.), Terra Scientific Publishing, 217-251.

Plumb, R.A. and R.C. Bell, 1982: Model of the quasi-biennial oscillation on an equatorial beta-plane. *Quart. J. Roy. Meteorol. Soc., 108,* 335-352.

Plumb, R.A. and A.D. McEwan, 1978: The instability of a forced standing wave in a viscous stratified fluid: a laboratory analogue of the quasi-biennial oscillation. *J. Atmos. Sci., 35,* 1827- 1839.

Reed, R.J., 1965: The present status of the 26-month oscillation, *Bull. Amer. Meteorol. Soc., 46,* 374-386.

Reed, R.J., W.J. Campbell, L.A. Rasmussen and D.G. Rogers, 1961: Evidence of a downward-propagating annual wind reversal in the equatorial stratosphere. *J.Geophys. Res, 66,* 813-818.

Salby, M., and P. Callaghan, 2000: Connection between the Solar Cycle and the QBO: The missing link. *J. Clim., 13,* 2652-2662.

Saravanan, R., 1990: A multiwave model of the quasi-biennial oscillation. *J. Atmos. Sci., 47,* 2465-2474.

Veryard, R.G. and R.A. Ebdon, 1961: Fluctuations in tropical stratospheric winds. *Meteorological Magazine, 90,* 127-143.

Wallace, J.M., 1973: The general circulation of the tropical lower stratosphere. *Rev. Geophys. Space Phys., 11,* 191-222.

altitude (km)

Equatorial T_0

$T_0 = 260\,°K$

ARDC

temperature (°K)

①

Pressure (hPa)

Zonal mean temperature (K)   April

②
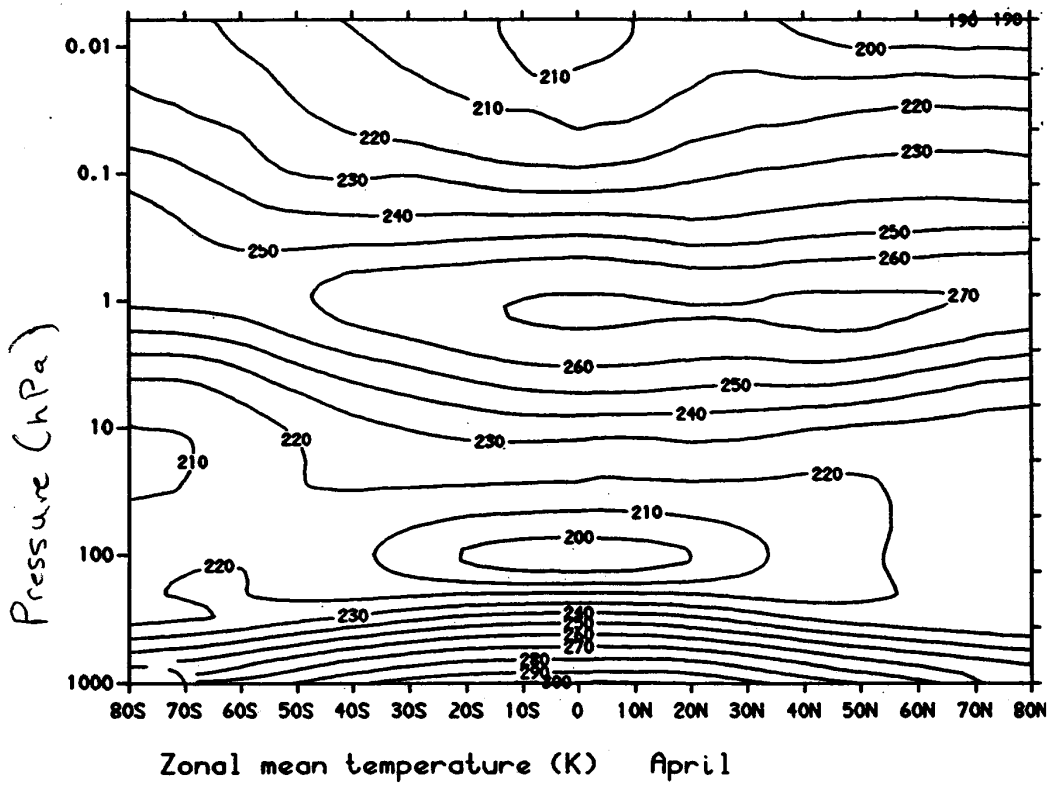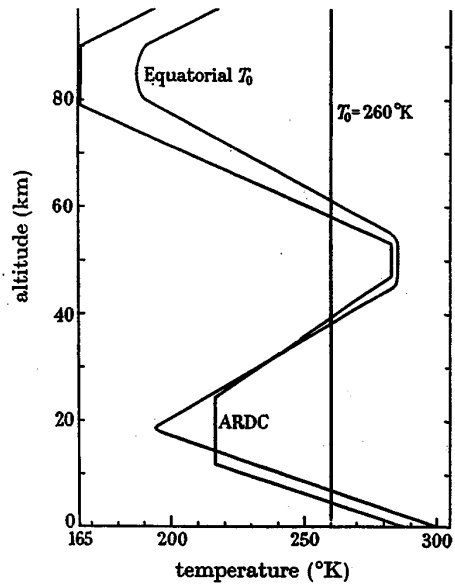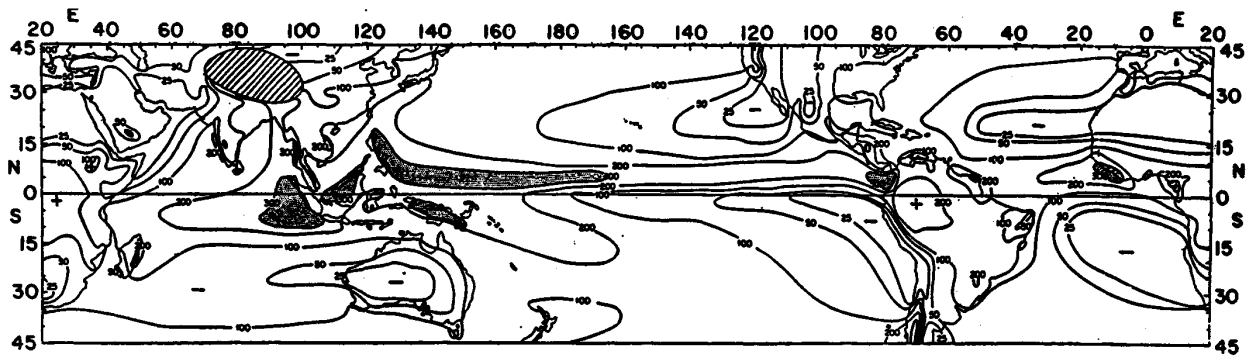
c: mean annual precipitation (cm) (...). Shaded: regions with more than 300 cm/year.

HALOE water vapor   January

HALOE water vapor   April

HALOE water vapor   July

HALOE water vapor   October
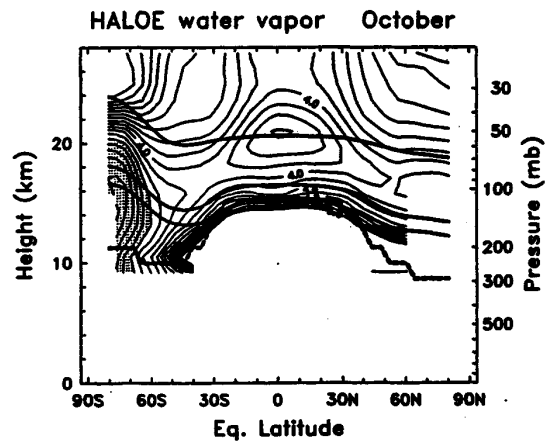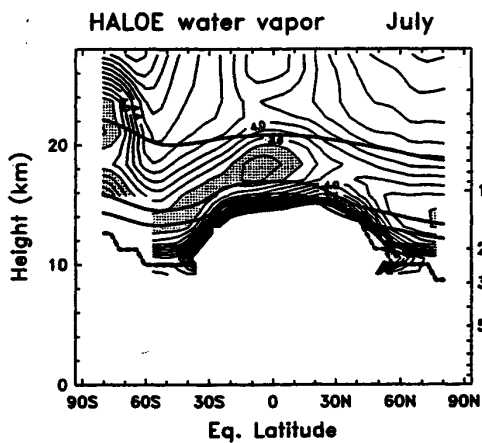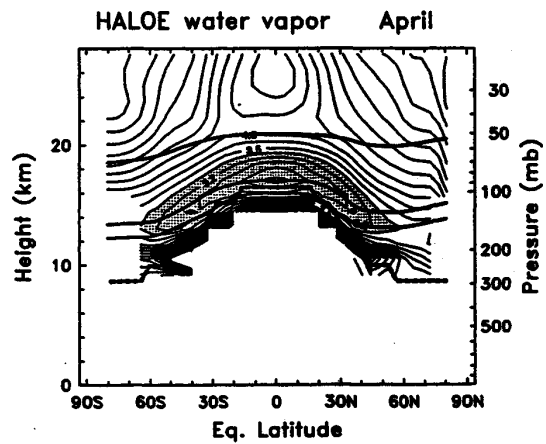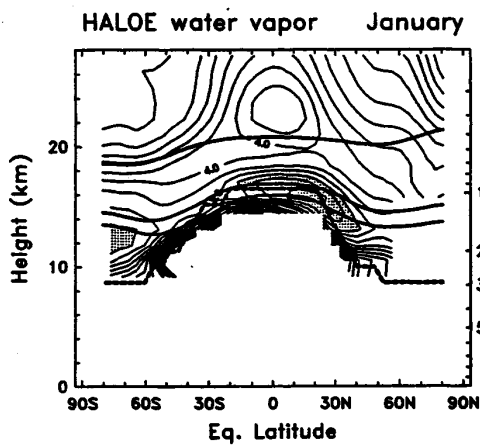
Meridional cross-sections of water vapour mixing ratio between the tropopause and ~28 km derived from HALOE measurements. Plots are shown for January, April, July and October, illustrating the seasonal cycle. For each month the dashed lines represent the tropopause, and the solid lines show the 380 K, 400 K, and 500 K isentropes.

Pressure (mb)

30

100

300

1000

Wave-driven

extratropical

"pump"

Large-scale
subsidence

Large-scale ascent

400
380
350
330

300

Two-way exchange
blocking anticyclones
cut-off cyclones
tropopause folds

Some
cumulonibus
clouds
penetrate
stratosphere

Pole

Equator

Latitude

⑤
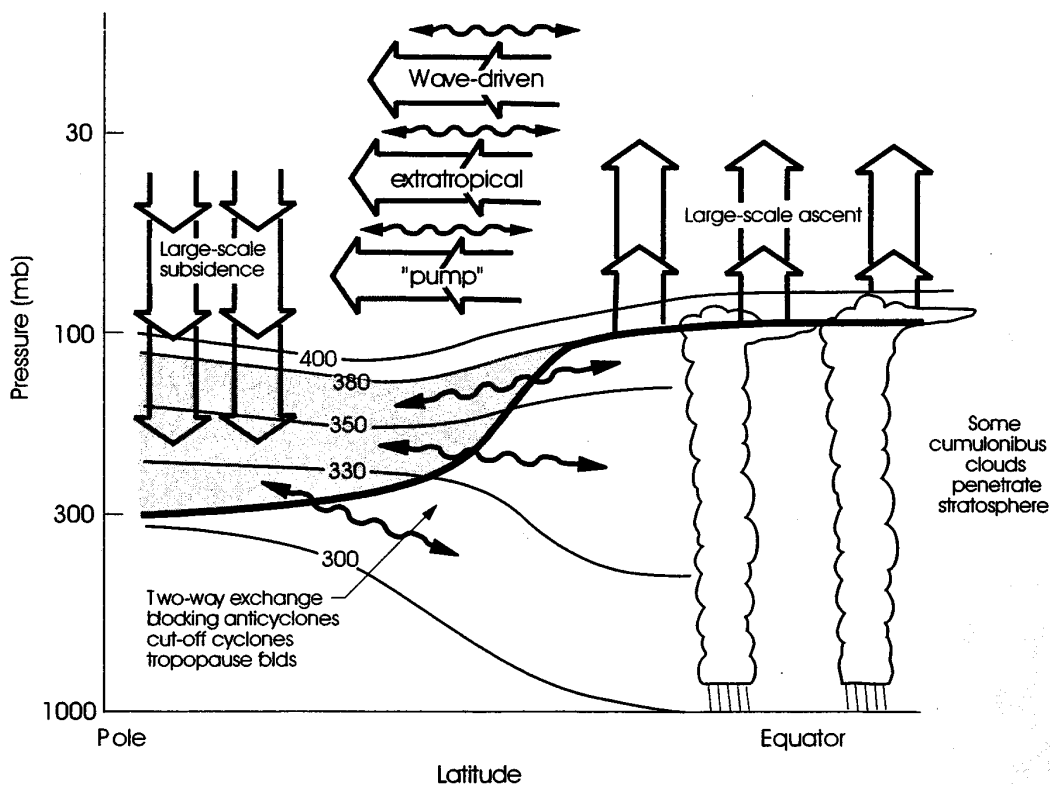
Dynamical Aspects of stratosphere-troposphere exchange.

The tropopause is shown by the thick line. Thin lines are isentropic or constant potential temperature surfaces labelled in Kelvins. Heavily shaded region is the "lowermost stratosphere" where isentropic surfaces span the tropopause and isentropic exchange by tropopause folding occurs. The region above the 380K surface is the "overworld", in which isentropes lie entirely in the stratosphere. Light shading in the overworld denotes wave-induced forcing (the extratropical "pump"). The wiggly double headed arrows denote meridional transport by eddy motions, which include tropical upper-tropospheric troughs and their cut-off cyclones as well as their midlatitude counterparts including folds. Not all eddy transports are shown; and the wiggly arrows are not meant to imply any two way symmetry. The broad arrows show transport by the global-scale circulation which is driven by the extratropical pump. This global scale circulation is the primary contribution to exchange across isentropic surfaces (e.g., the ~380 K surface) that are entirely in the overworld. (Holton et al., Reviews of Geophysics, 1995).

Trend over Boulder, CO

Water Vapor
1981–2000

Altitude [km]

Trend [%/year]
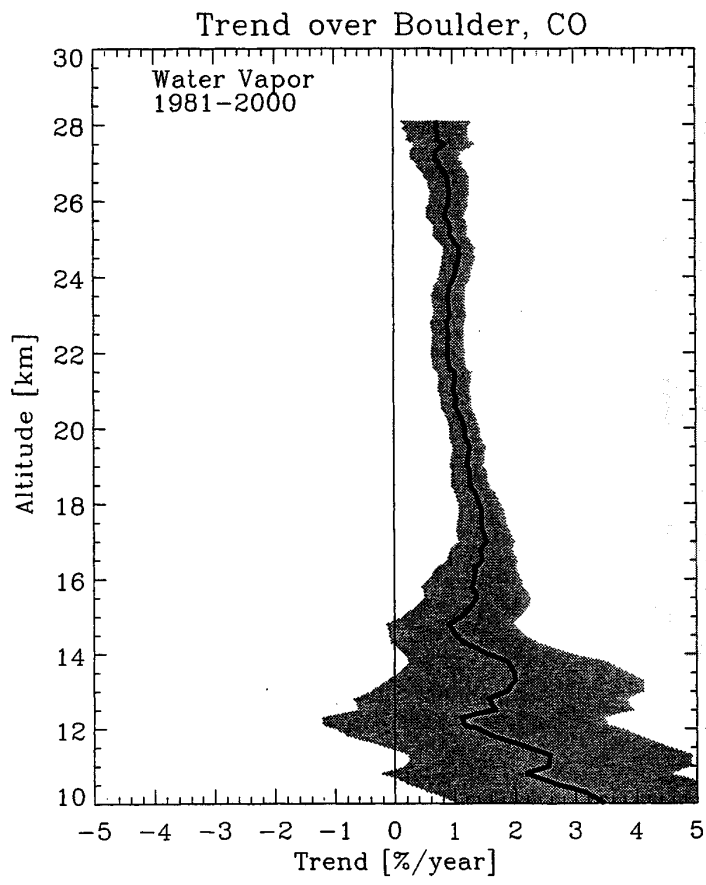
The linear trend of water vapour mixing ratio (percent per year) and 95% confidence interval (shaded area) as a function of altitude over Boulder. Significant increases of about 1% per year are found at all altitudes above 16 km.
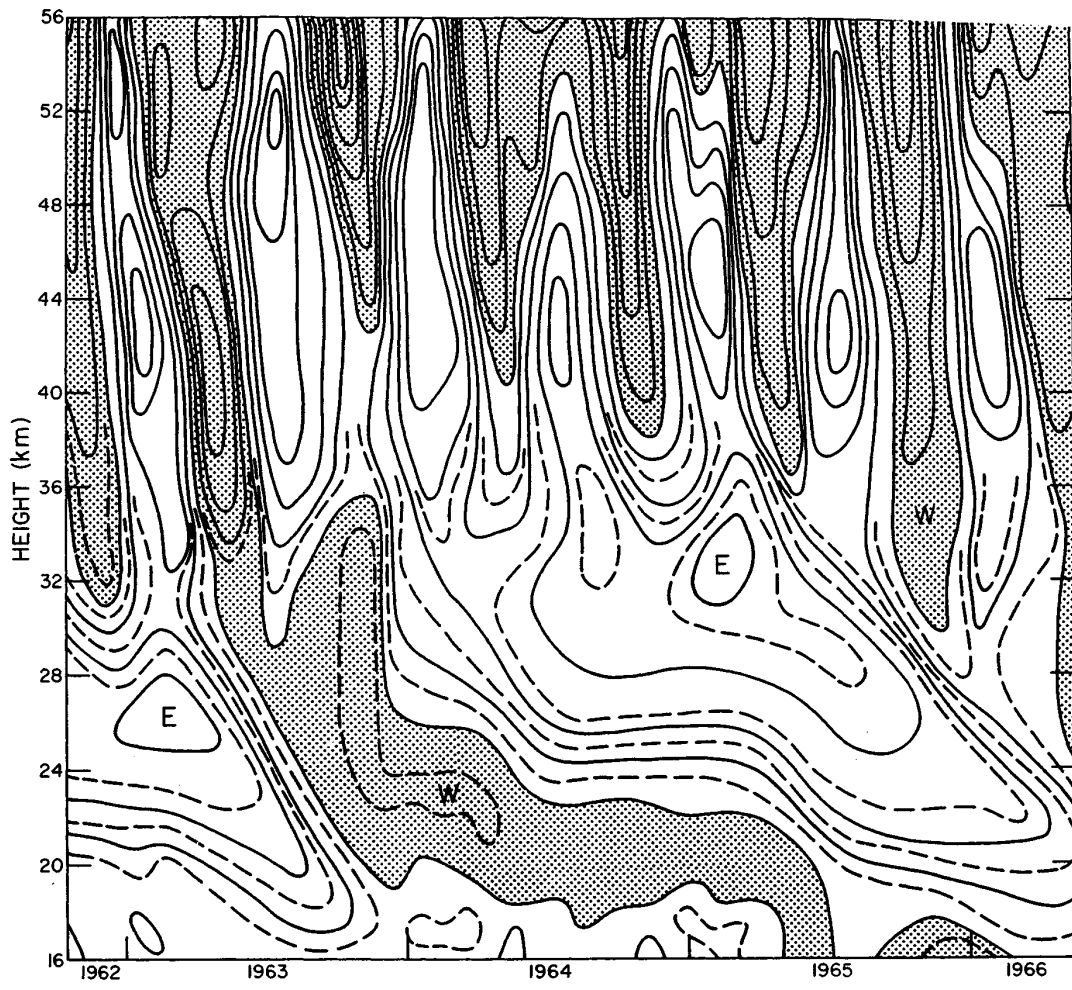
Time–height section of zonal wind in the vicinity of the equator based on monthly averaged data. Solid lines have been drawn at intervals of 10 m s^{-1}. Shaded regions denote flow from west to east, and the letters W denote maxima of such *westerly* flow. E's denote maxima of easterly (east to west) flow. At the higher levels there is a prominent semiannual oscillation while below 35 km there is a longer-term variability associated with the quasi-biennial oscillation. [From Wallace, *Rev. Geophys. and Space Phys.*, **11**, 196 (1973), copyrighted by American Geophysical Union.]

Geomagnetic Latitude

Geomagnetic (350km Apex) Latitudes

Based on modified apex coordinates at 350km altitude
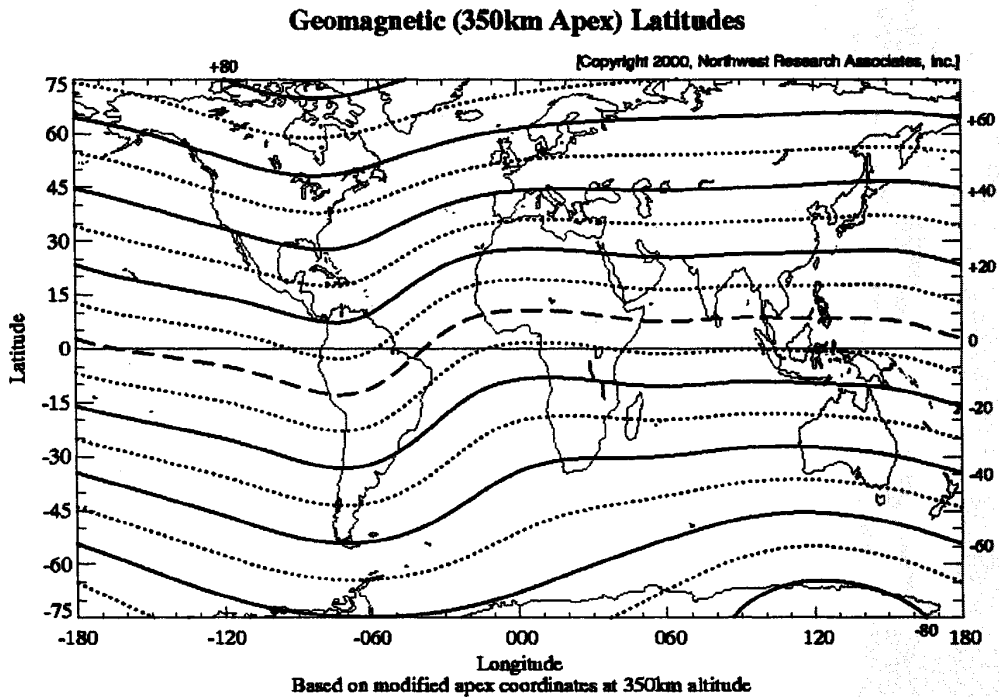
This maps shows lines of constant geomagnetic latitude based on apex geomagnetic coordinates referenced to an altitude of 350km. The geomagnetic equator is indicated by a dashed line. The coordinates were calculated using the IGRF-1985 geomagnetic field model updated to epoch 1990.0.

Definitions
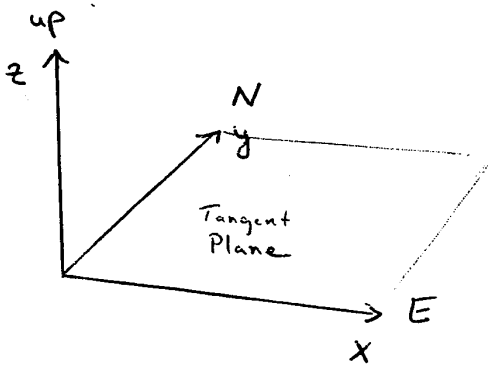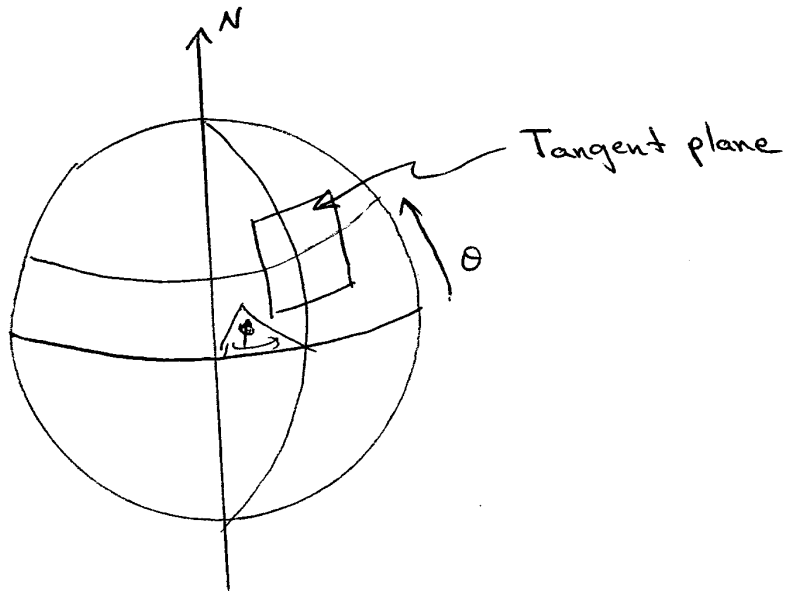
$$u \equiv \frac{dx}{dt} \equiv \text{"westerly wind"}$$

$$v \equiv \frac{dy}{dt} \equiv \text{"southerly wind"}$$

$$w \equiv \frac{dz}{dt} \equiv \text{"vertical wind"}$$
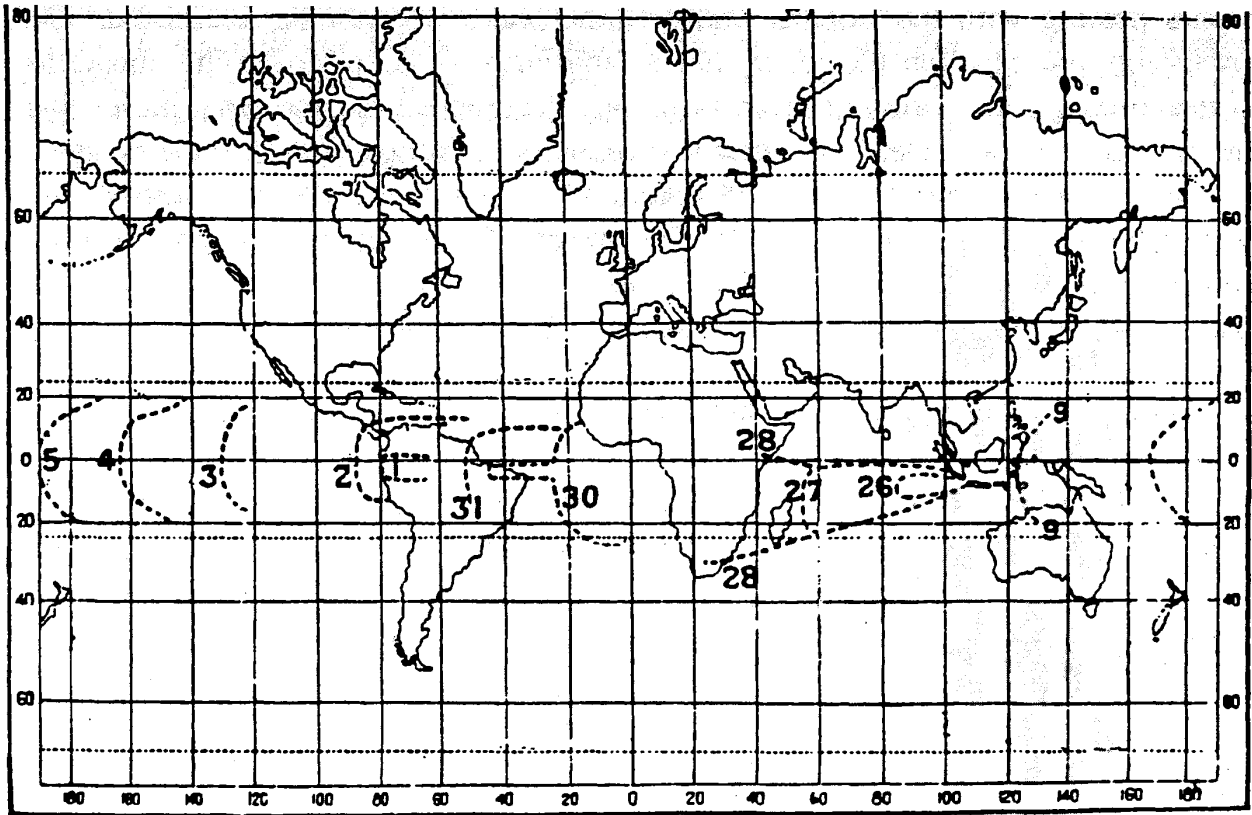
The spread of the optical phenomena observed after the eruption of Mt. Krakatoa on 26 August 1883. The dotted lines give the western boundary of the region where the phenomena had been observed on successive days, 26 August, 27 August ... 9 September. Reproduced from Russell (1888).

Singapore (1.3°N) 30 mb Zonal Wind
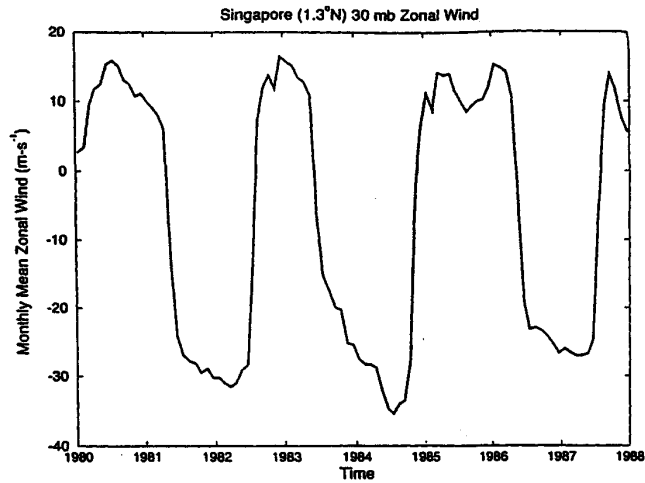
Time series of the monthly-mean zonal wind measured by balloons at Singapore during the period 1980–88.
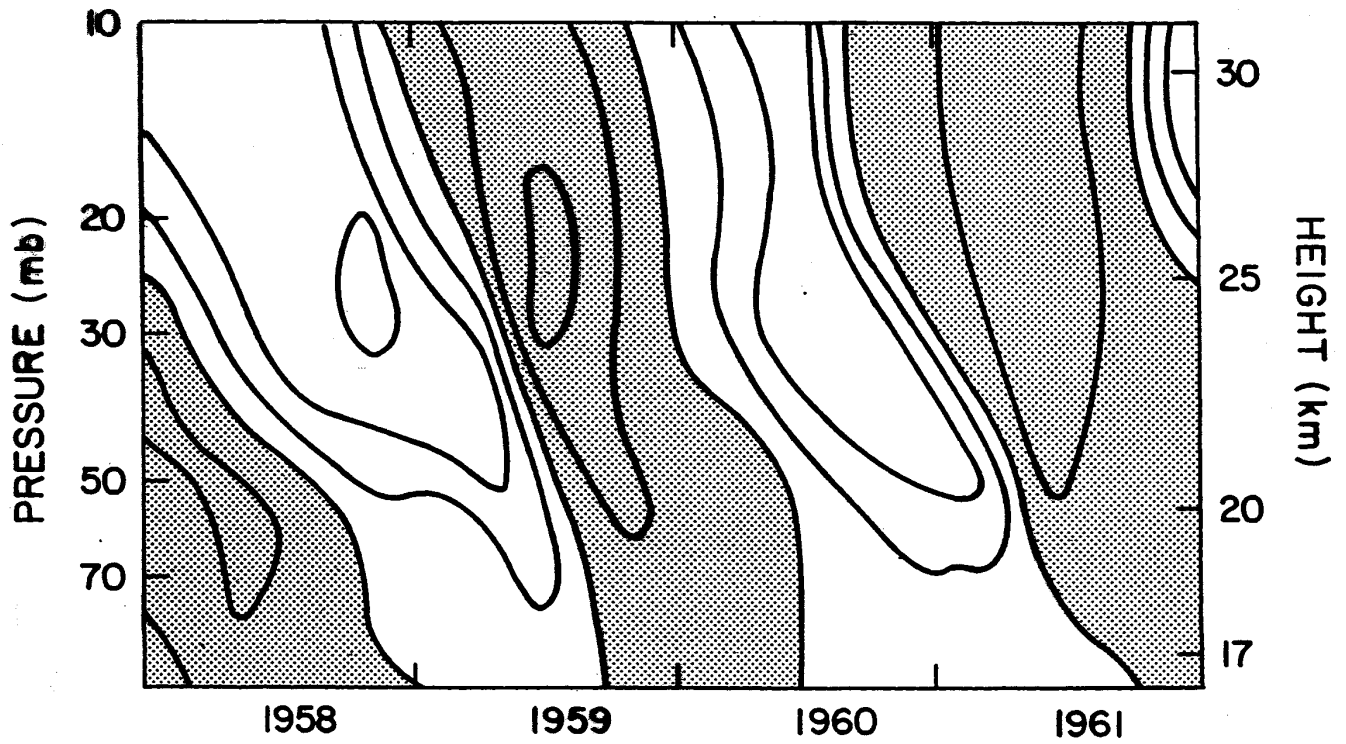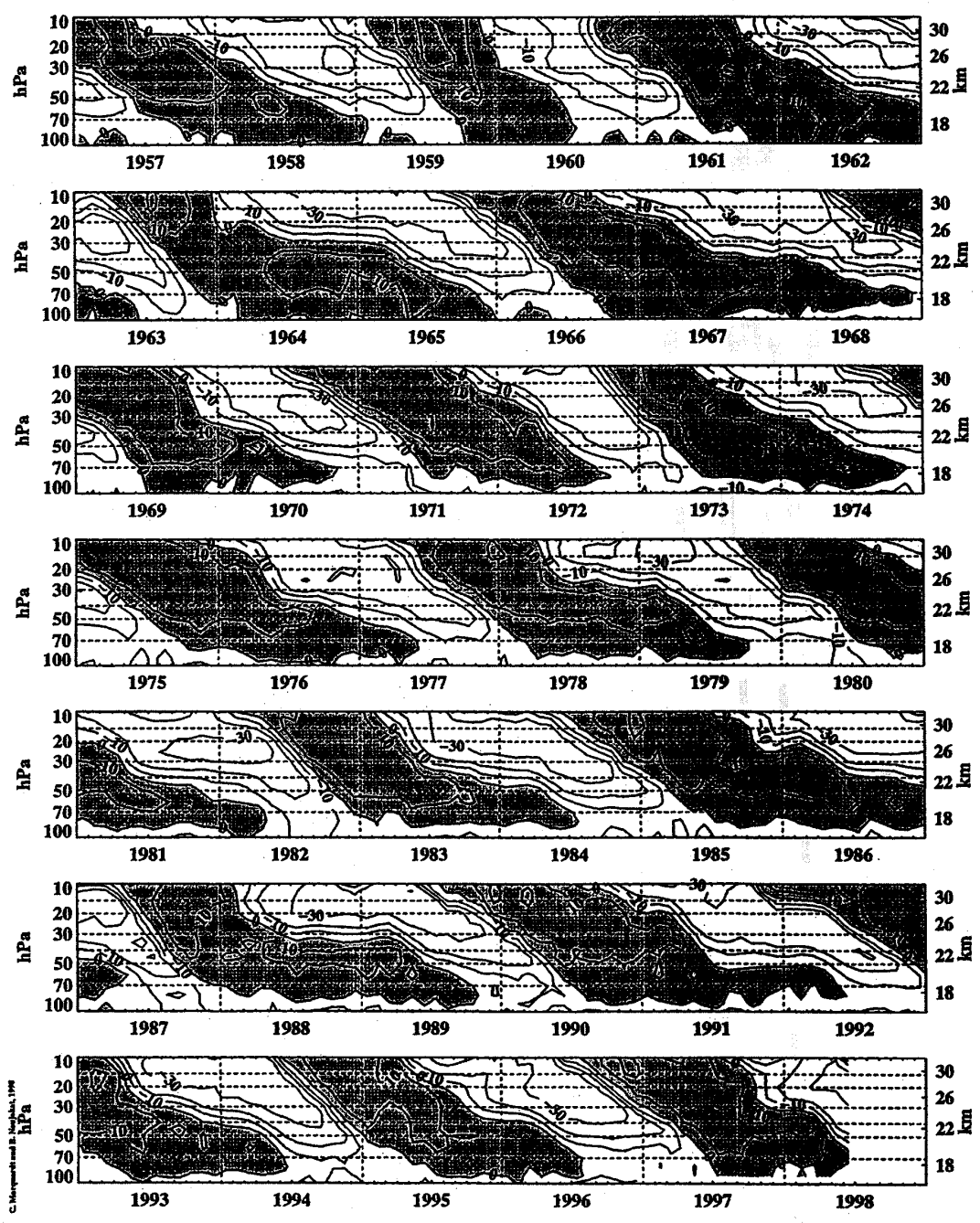
Time-height section of the monthly-mean wind at stations near the equator. Results represent observations from Canton Island (2.8°S, 171.7°W) during 1957–1967, Gan (0.7°S, 73.1°E) during 1967–1975, and Singapore (1.4°N, 103.9°E) during 1976–1998. Westerly winds are shaded and the contour interval is 10 m s^{-1}. Figure provided by B. Naujokat.
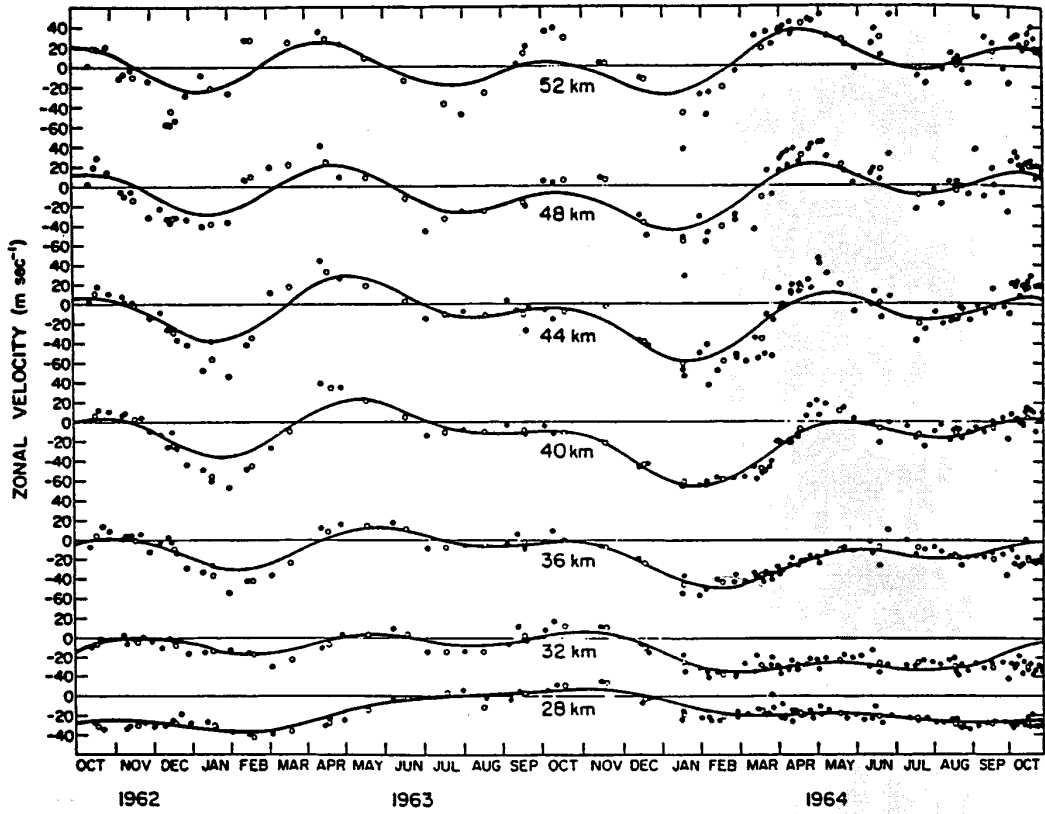
Zonal wind measurements taken at Ascension island (7.9°S) during the period October 1962 through October 1964. The solid circles show individual measurements and the open circles are monthly means for months when there was more than one measurement available. Reproduced

Equatorial Zonal Wind, Deseasoned Monthly Means

Equatorial Zonal Wind, 9-48 Month Bandpass
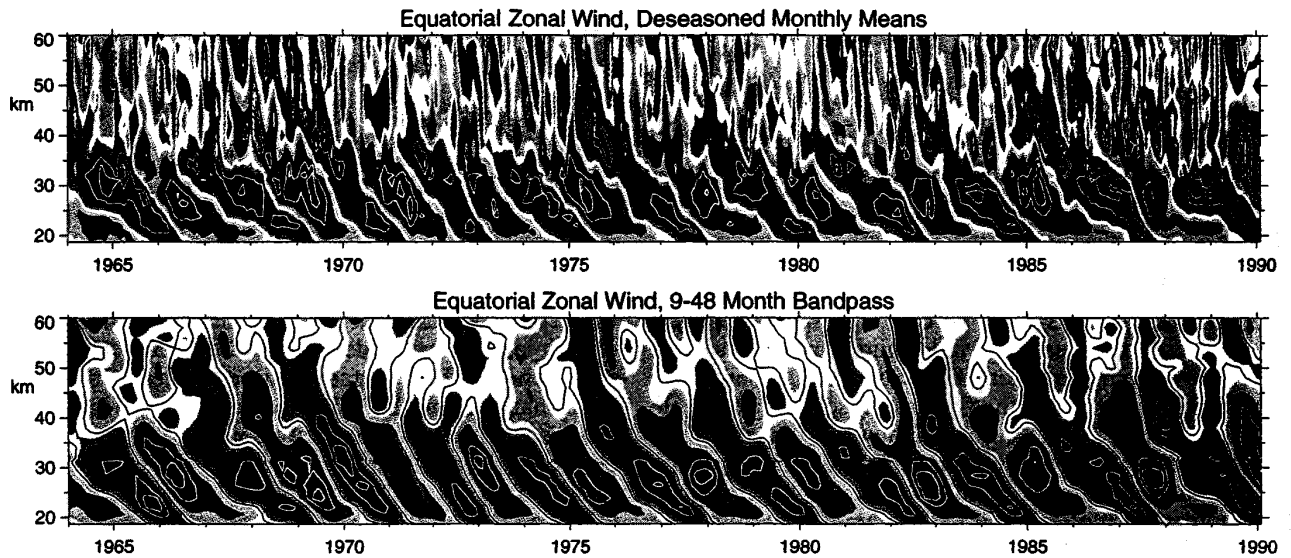
. (top) Time-height section of the monthly-mean zonal wind component (m s^{-1}), with the seasonal cycle removed, for 1964–1990. Below 31 km, equatorial radiosonde data are used from Canton Island (2.8°N, January 1964 to August 1967), Gan/Maledive Islands (0.7°S, September 1967 to December 1975), and Singapore (1.4°N, January 1976 to February 1990). Above 31 km, rocketsonde data from Kwajalein (8.7°N) and Ascension Island (8.0°S) are shown. The contour interval is 6 m s^{-1}, with the band between −3 and +3 unshaded. Red represents positive (westerly) winds. After *Gray et al.* [2001]. In the bottom panel the data are band-pass filtered to retain periods between 9 and 48 months.

(15)
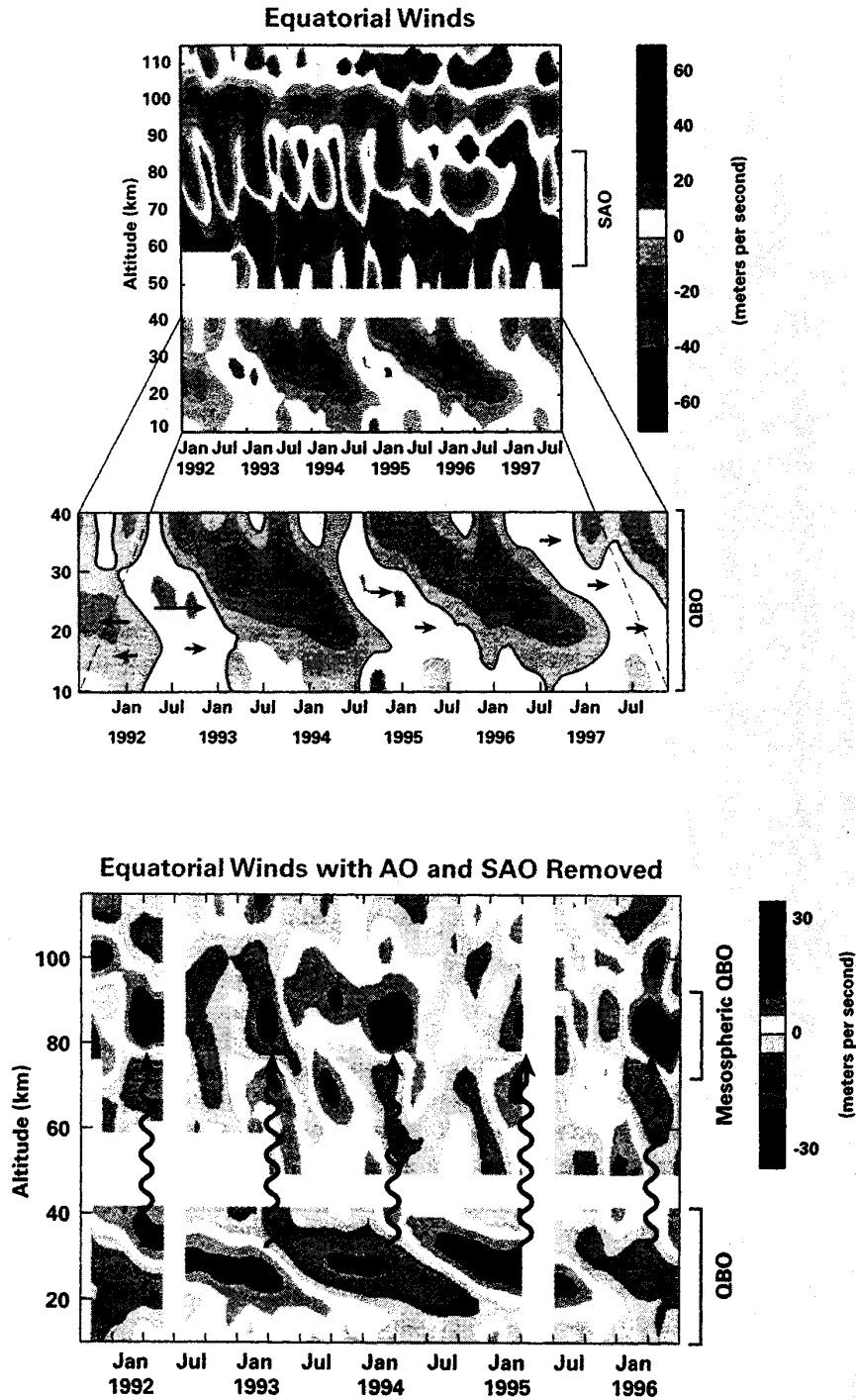
(top) High Resolution Doppler Imager (HRDI) measurements of the zonally averaged zonal wind in the tropical stratosphere and mesosphere from 1992 to 1998. The lower panel shows the QBO from 20 to 40 km as descending easterly (green to blue) and westerly (red to yellow) winds. In the lower mesosphere (60–80 km) the wind structure is dominated by the semiannual oscillation (SAO). (bottom) Removing the SAO and the annual oscillation (upper panel) shows that the influence of the QBO extends into the mesosphere (80 km). Mesospheric wind changes coincide with the change of the QBO winds near 30 km. This coupling between the mesosphere and the stratosphere is believed to be caused by small-scale upward propagating gravity waves, indicated by wavy arrows. From the UARS brochure, modified from the original provided by M. Burrage and D. Ortland. Courtesy M. Schoeberl.
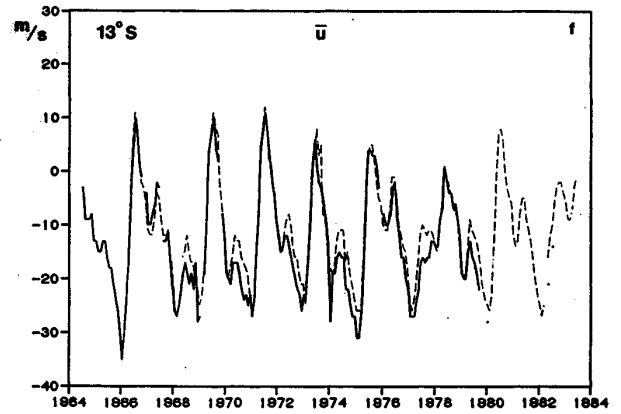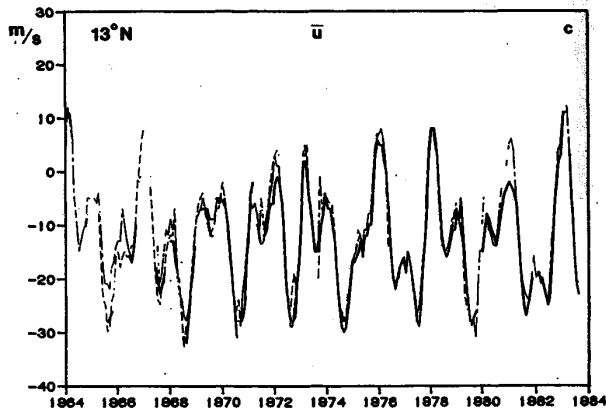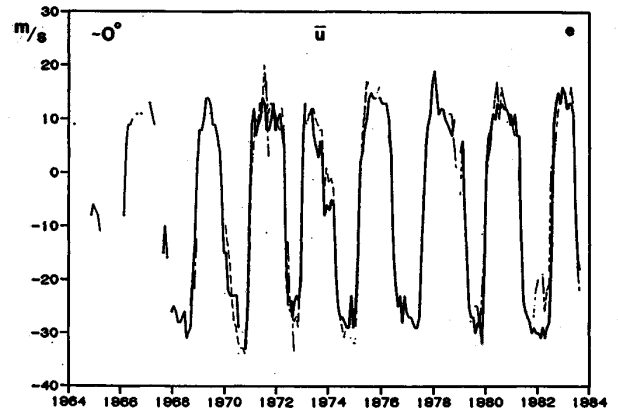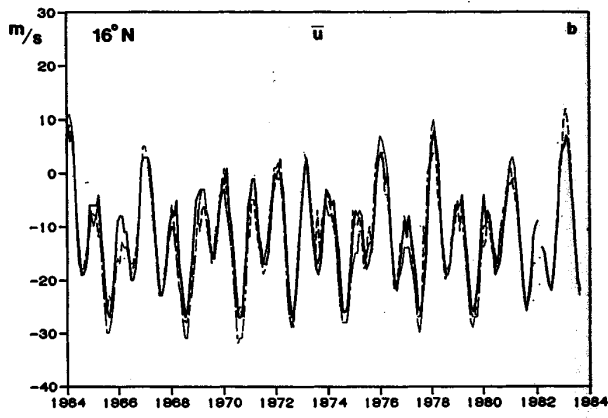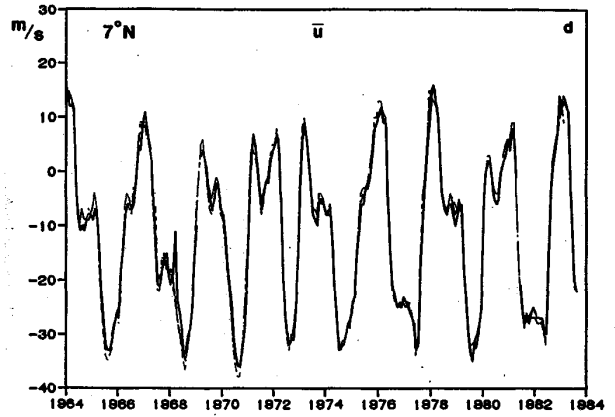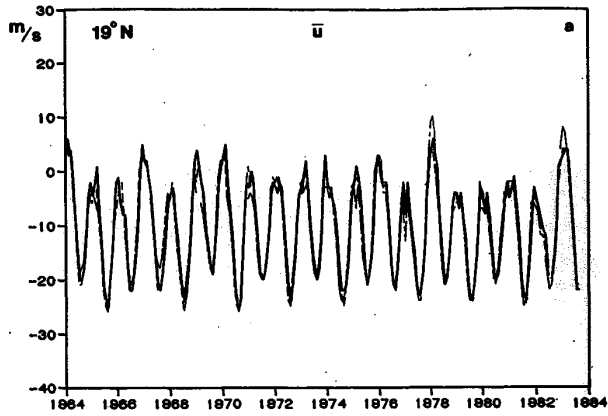
Time series of 30 mb zonal wind at various latitudes, comparing stations of similar latitude but different longitude. Positive values denote westerlies. (Refer to Table 1 for exact station locations.)

17
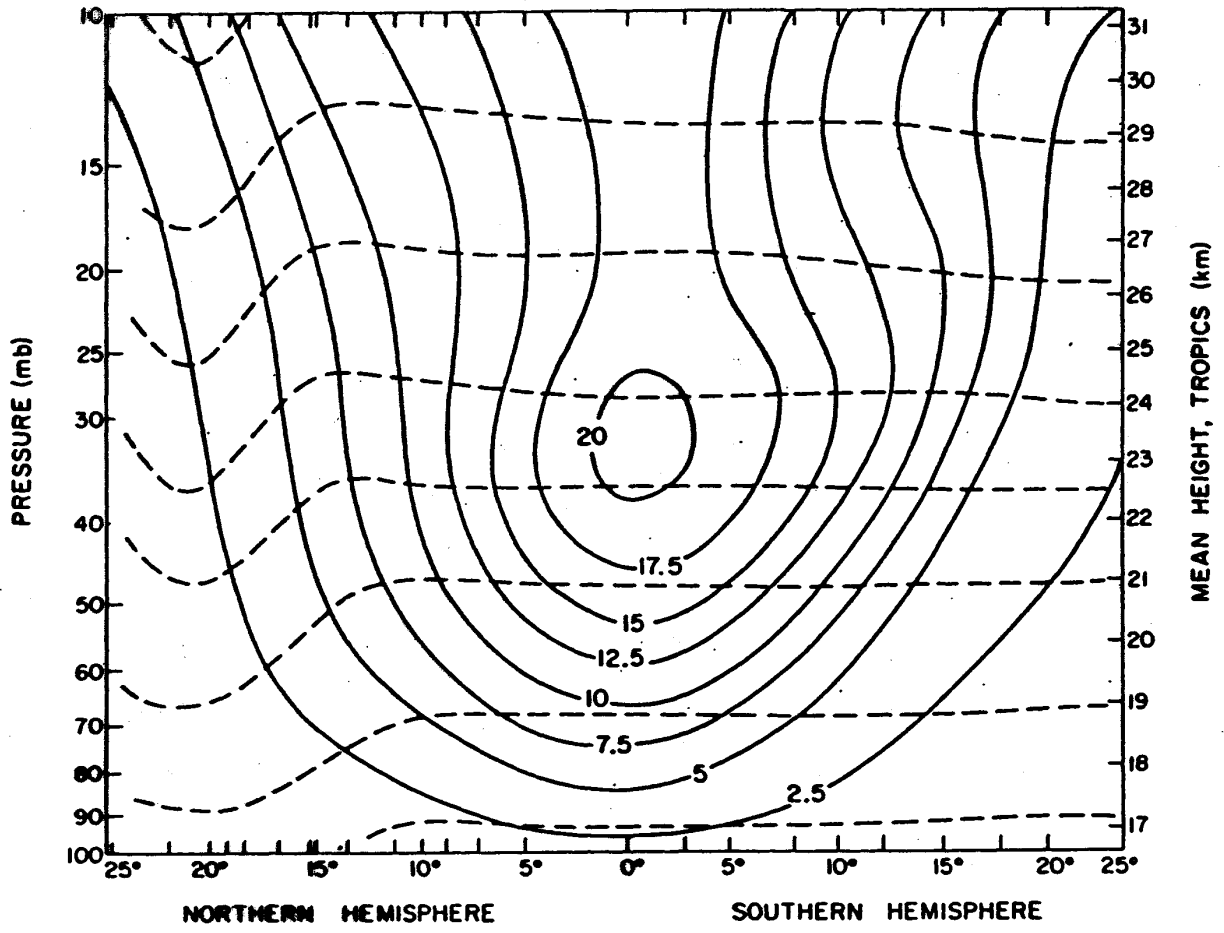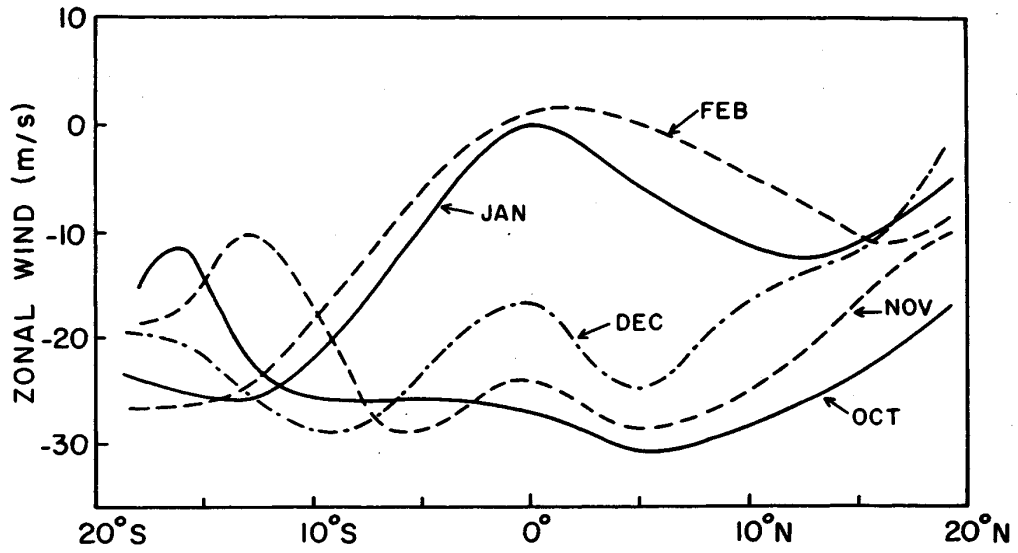
Profiles of the mean zonal wind at 30 mb (deduced from balloon observations) for each month from October 1979 through February 1980.
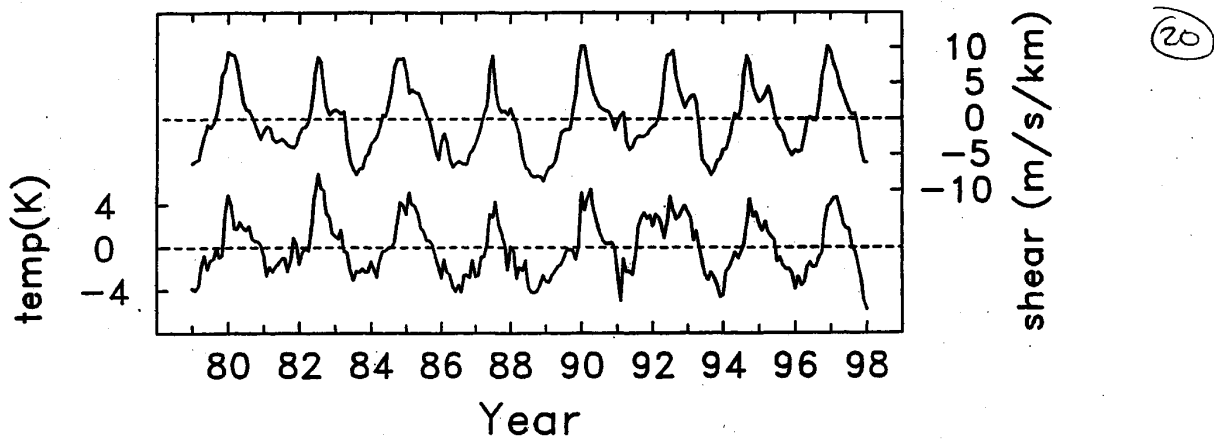
Equatorial temperature anomalies associated with the QBO in the 30- to 50-hPa layer (bottom I vertical wind shear (top curve).
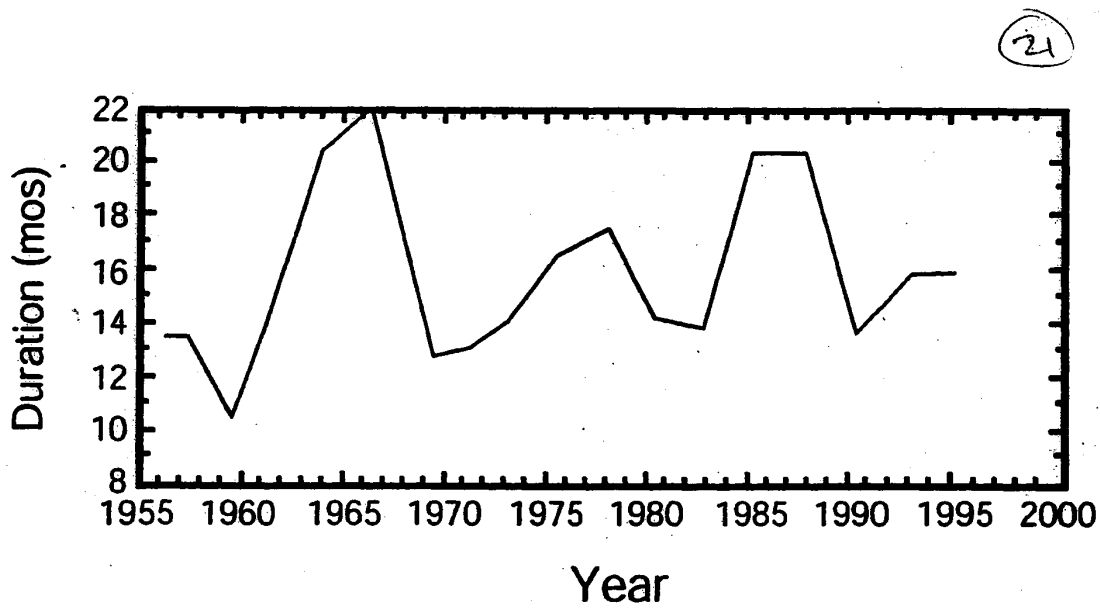
Duration of equatorial westerlies as a function of year.

50hPa E-W

NUMBER OF TRANSITIONS

Top panel (J F M A M J J A S O N D):

- J: 95, 77
- M: 99
- A: 55, 85
- M: 97, 90, 73, 71, 69, 61
- J: 80, 66, 57
- J: 75
- A: 59
- O: 87, 82, 63
- D: 92

50hPa W-E

Bottom panel (J F M A M J J A S O N D):

- J: 76
- A: 87, 54
- M: 98, 96, 94, 84, 68, 56
- J: 89, 79, 70, 60
- J: 91, 74, 72, 65
- S: 58
- N: 81, 62
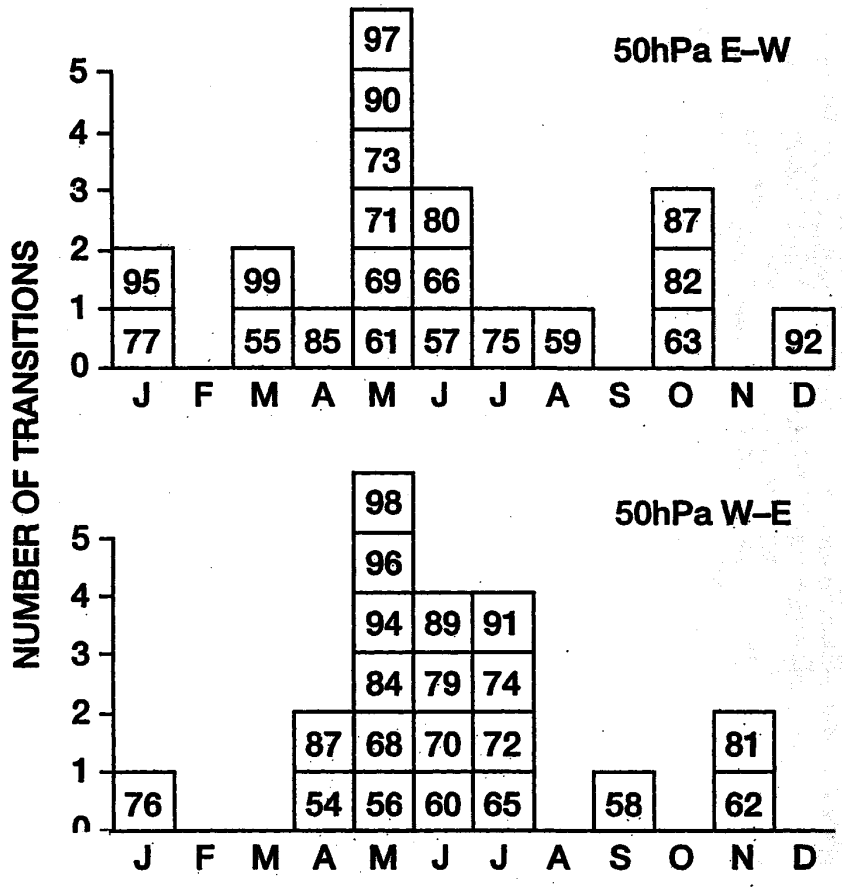
Histograms of the number of transitions (zero crossings) at 50 hPa grouped by month. Individual years are listed in the boxes. Easterly to westerly transitions are displayed in the top panel, while westerly to easterly transitions are shown in the bottom panel. After *Pawson et al.* [1993].
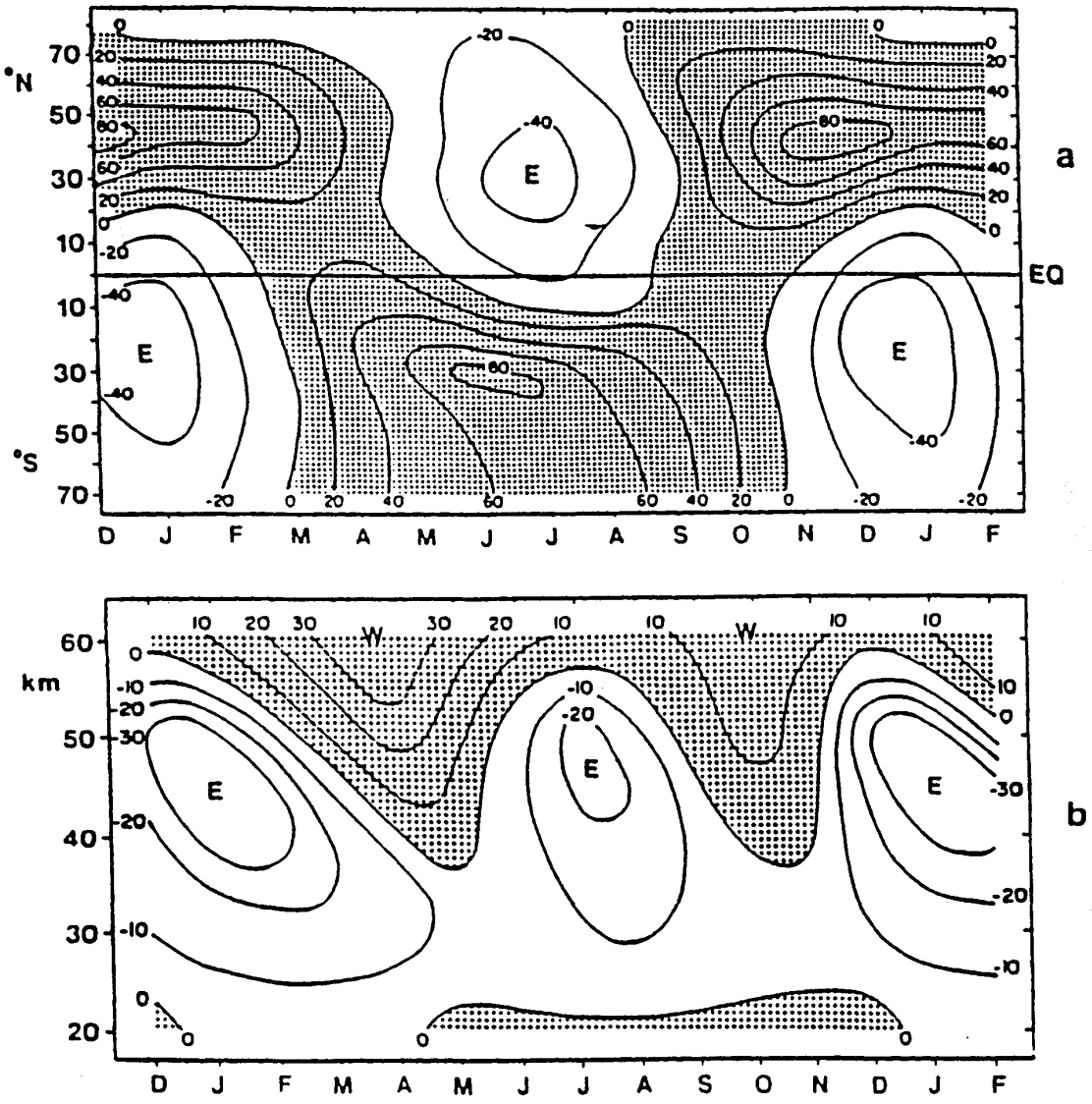
(top) Latitude-time section of the climatological annual march of zonal-mean zonal winds at 50-km height determined from rocketsonde observations at several stations. Contour interval is 20 m s^{-1} and regions of westerlies are shaded. (bottom) Altitude-time section of the annual march of equatorial zonal wind determined from interpolation of observations at Kwajalein (8.7°N) and Ascension Island (7.9°S). Contour interval is 10 m s^{-1} and regions of westerlies are shaded. Reproduced from Delisi and Dunkerton (1988b) and based on an earlier figure from Belmont et al. (1975).
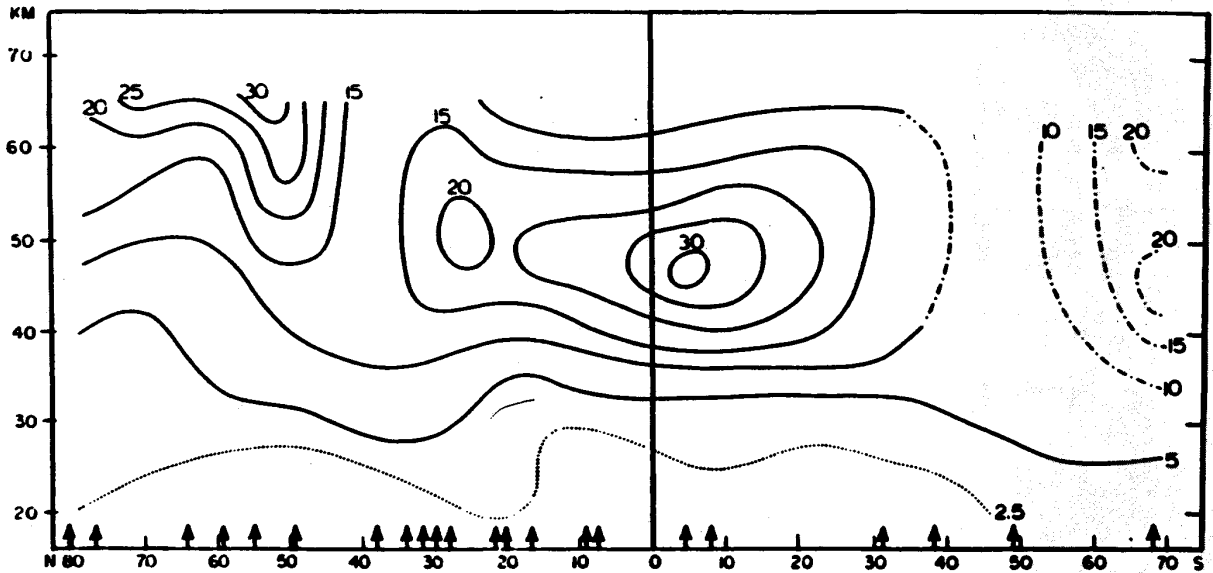
(Top) The amplitude of the quasi-biennial oscillation of the zonal wind as a function of height and latitude determined by Belmont et al. (1974) from rawind-sonde and meteorological rocket data at 24 stations. The amplitude was computed by fitting a 29 month harmonic to the data. Contour labels are in m/sec. The arrows at the bottom show the station locations. (Bottom) The amplitude of the semiannual oscillation of the zonal wind. Also reproduced from Belmont et al. (1974).
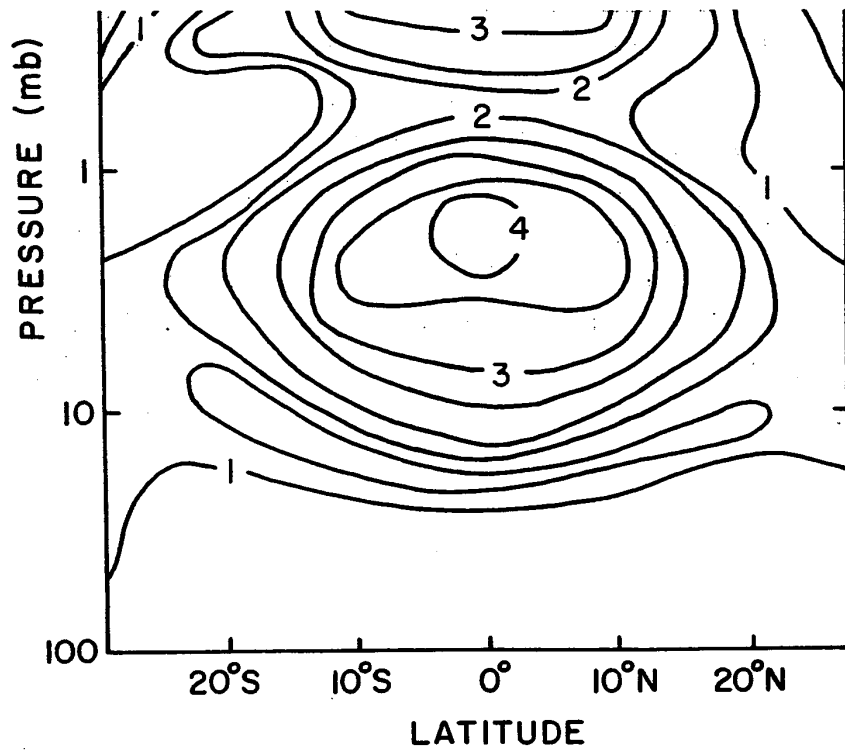
Amplitude of the semiannual harmonic of the zonally-averaged
temperature
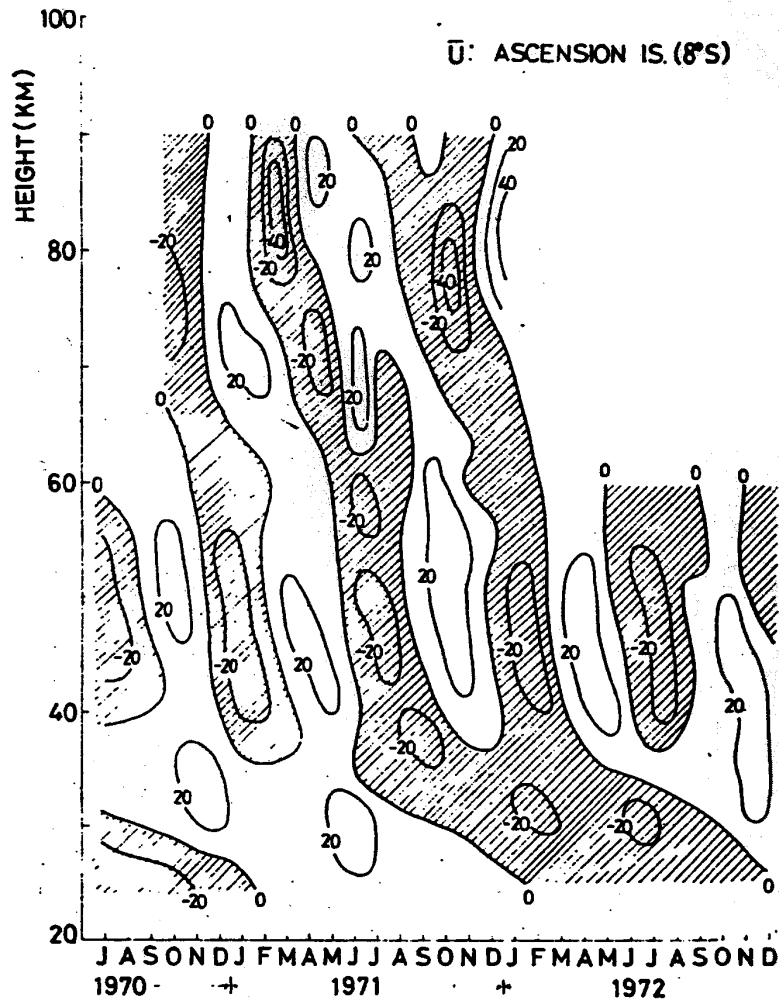
Vertical time-section of the monthly mean zonal wind at Ascension Island (8°S, 14°W) for the period July 1970–December 1972. The mean and annual component have been removed. Units are m s⁻¹ and the easterlies are shaded.
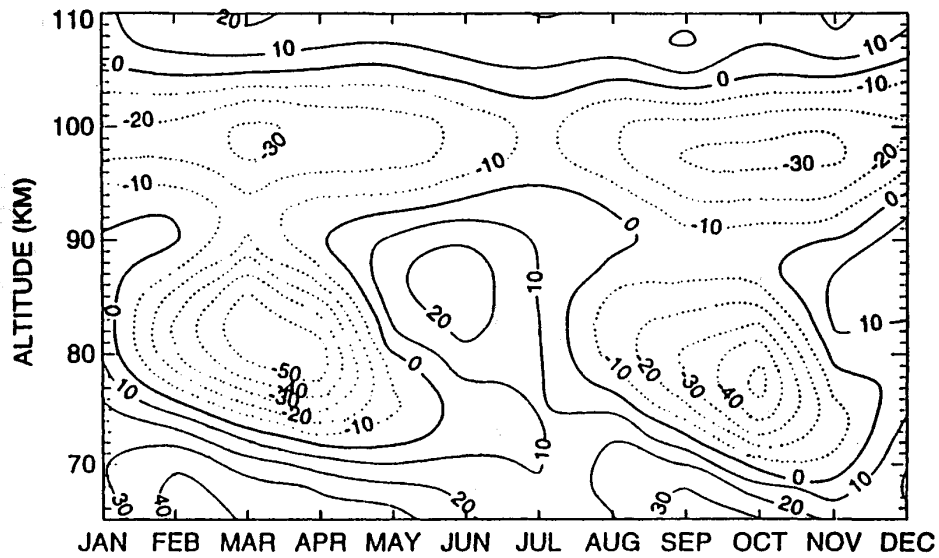
Annual march of the zonally-averaged equatorial zonal wind measured by the HRDI Doppler radiometer. The contour intervals is 10 m s^{-1} and dashed contours denote easterly winds. Reproduced from Garcia et al. (1997).
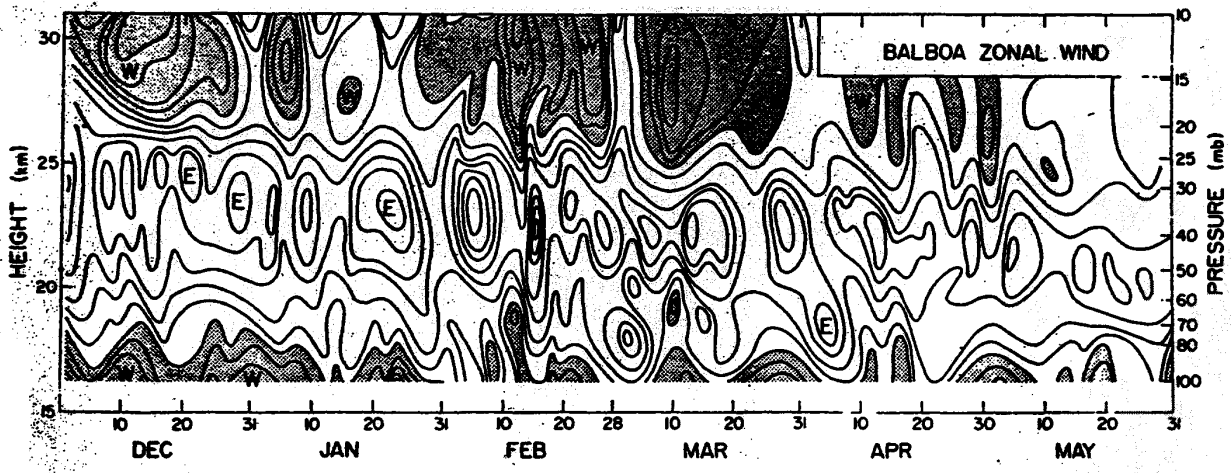
Time-height section of zonal wind at Balboa, Canal Zone (9°N). Isotachs are placed at intervals of 5 m sec^{-1}. Westerlies are shaded.
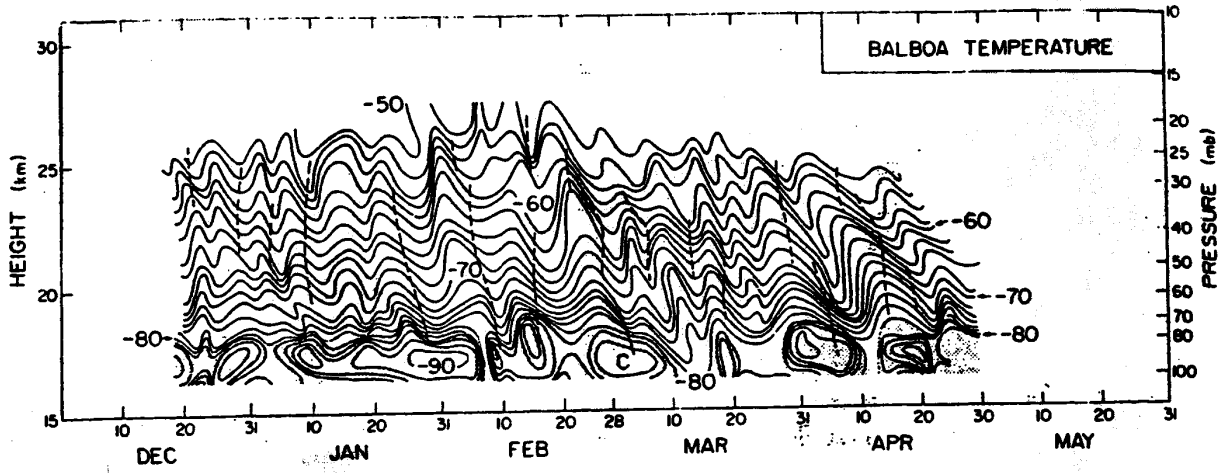
Time-height section of temperature at Balboa. Isotherms are placed at intervals of 2°C. Temperatures below —80°C are shaded. Dashed lines represent axes of the more prominent easterly fluctuations

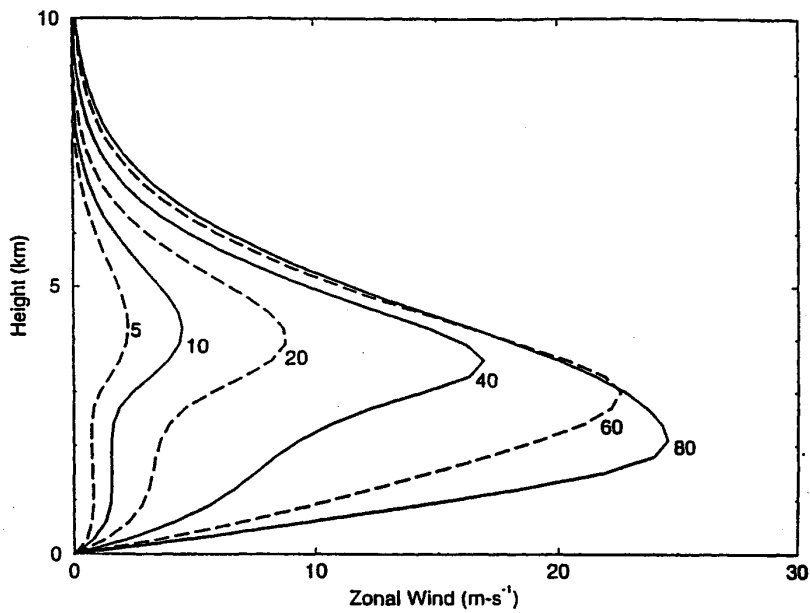2-DAY DIFFERENCE   (Feb.17-19, 1971)

(b) $P_U(\omega)\omega$ $[m^2 s^{-2}]$
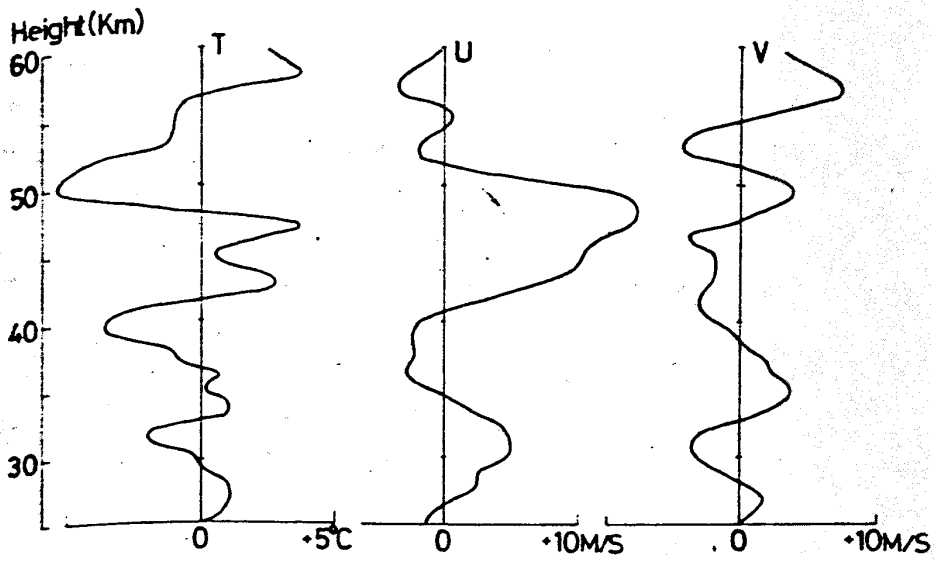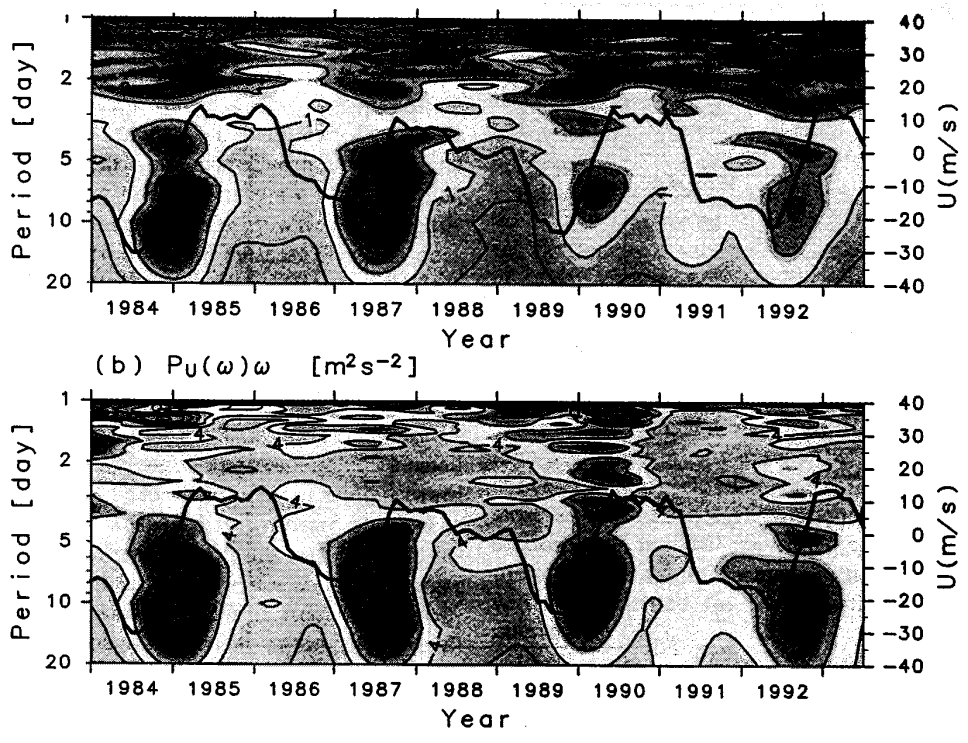
. Power spectra for (a) T and (b) u fluctuations at Singapore as a function of time, averaged over 20–25 km. Contour interval 0.5 K^2, and 2 $(m\ s^{-1})^2$, respectively.
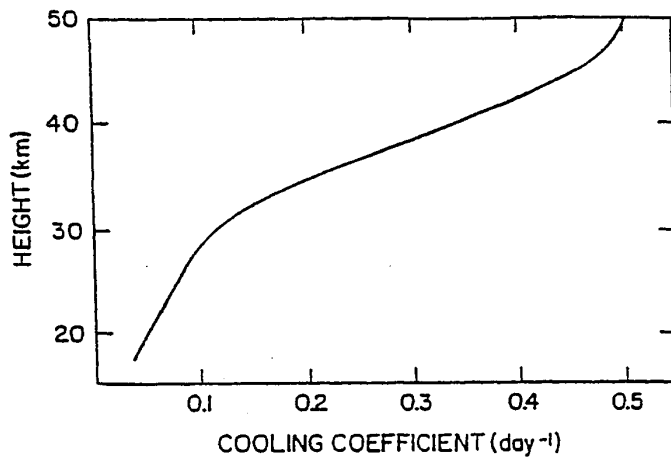
A reasonable representation of the damping rate of temperature perturbations due to radiative effects in the stratosphere. appropriate for temperature perturbations with long vertical scales. Reproduced from Hamilton (1982b) and based on the radiative-photochemical results of Blake and Lindzen (1973).

The mean zonal wind in a simple Boussinesq one-wave Plumb model plotted at 5, 10, 20, 40, 60 and 80 days of integration starting from zero mean wind. The parameters employed are $F(z = 0) = 0.02 \text{ m}^2 \text{ s}^{-2}$, $k = 2\pi/4 \times 10^7 \text{m}^{-1}$, $k/\omega = 30 \text{ m s}^{-1}$, mean flow diffusivity 0.3 m^2 s^{-1}, $N = 0.02 \text{ s}^{-1}$, $\alpha = 0.01 \text{ day}^{-1}$ for $z < 3$ km and $\alpha = 0.01 (1 + 3.3z) \text{ day}^{-1}$ for $z > 3$ km.
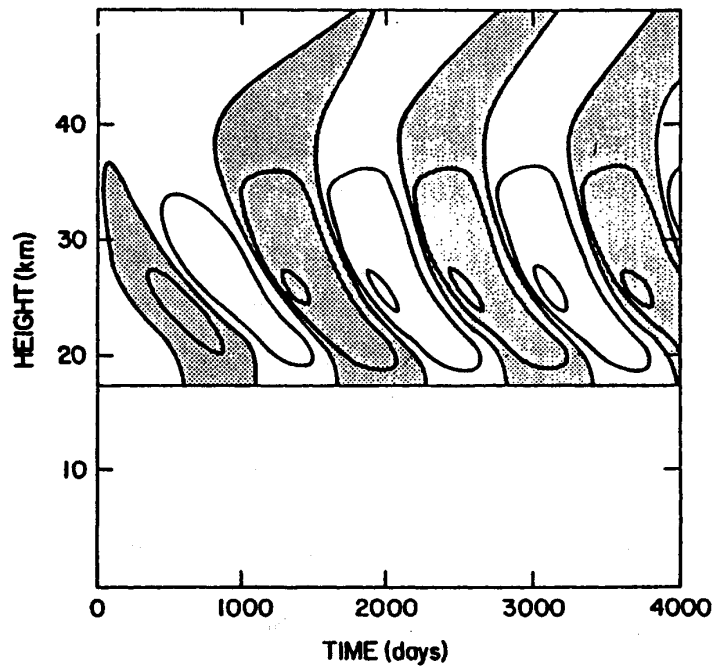
Height-time evolution of the mean flow in a two-wave Plumb model. The model employed is a version that takes into account compressibility. The model is forced with two waves with phase $+25$ m s^{-1} and -25 m s^{-1} and the wave fluxes are specified at the lower boundary located at 17-km height. The contour interval is 10 m s^{-1} and regions of negative wind are shaded. Reproduced from Hamilton (1982b), where further details can be found.
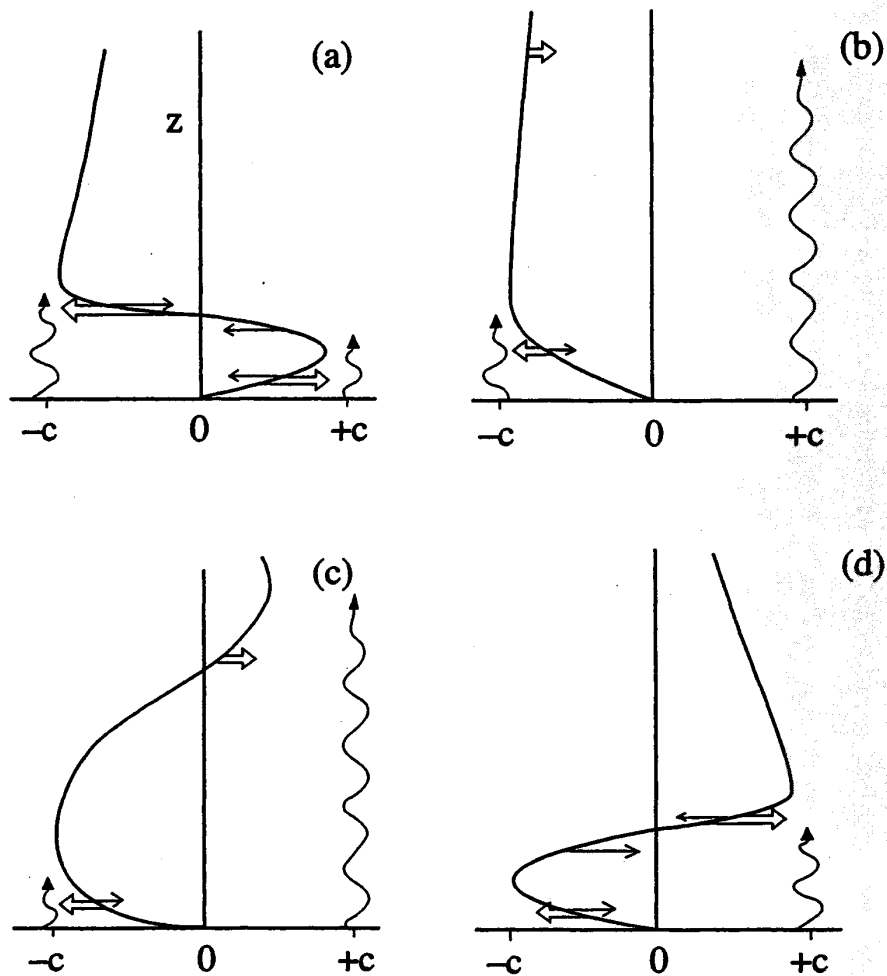
Schematic representation of the evolution of the mean flow in *Plumb*'s [1984] analog of the QBO. Four stages of a half cycle are shown. Double arrows show wave-driven acceleration, and single arrows show viscously driven accelerations. Wavy lines indicate relative penetration of eastward and westward waves. After *Plumb* [1984].
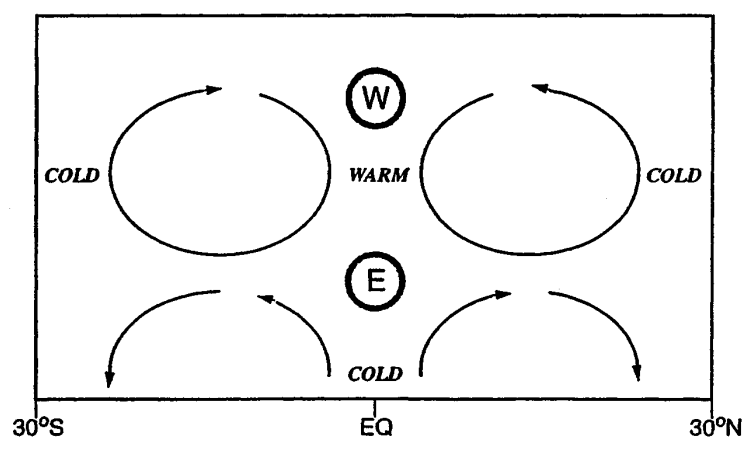
Schematic view of how the QBO may affect the mean meridional circulation in the tropical stratosphere. The "E" and "W" refer to the maximum easterly and westerly zonal winds, and the peak warm and cold QBO anomalies at the equator are also marked. Adapted from Reed (1965).